

# A gridded dataset of consumptive water footprints, evaporation, transpiration, and associated benchmarks related to crop production in China during 2000-2018

Wei Wang<sup>1,2</sup>, La Zhuo<sup>1,2,3\*</sup>, Xiangxiang Ji<sup>4</sup>, Zhiwei Yue<sup>4</sup>, Zhibin Li<sup>1,2</sup>, Meng Li<sup>4</sup>, Huimin Zhang<sup>4</sup>, Rong Gao<sup>4</sup>, Chenjian Yan<sup>4</sup>, Ping Zhang<sup>4</sup>, Pute Wu<sup>1,2,3\*</sup>

<sup>1</sup>Institute of Soil and Water Conservation, Chinese Academy of Sciences and Ministry of Water Resources, Yangling 712100, China

<sup>2</sup>University of Chinese Academy of Sciences, Beijing 100049, China

<sup>3</sup>Institute of Soil and Water Conservation, Northwest A&F University, Yangling 712100, China

<sup>4</sup>College of Water Resources and Architectural Engineering, Northwest A&F University, Yangling 712100, China

*Correspondence to:* La Zhuo (zhuola@nwafu.edu.cn; lzhuo@ms.iswc.ac.cn), Pute Wu (gjzwpt@vip.sina.com).

**Abstract.** Evapotranspiration over crop growth period, also referred to as the consumptive water footprint of crop production (WFCP), is an essential component of the hydrological cycle. However, the existing high-resolution consumptive WFCP datasets do not distinguish between soil evaporation and crop transpiration and disregard the impacts of different irrigation practices. This restricts the practical implementation of existing WFCP datasets for precise crop water productivity assessments, agricultural water-saving evaluations, the development of sustainable irrigation techniques, cropping structure optimisation, and crop-related interregional virtual water trade analysis. This study establishes a 5-arcmin gridded dataset of monthly green and blue WFCP, evaporation, transpiration, and associated unit WFCP benchmarks for 21 crops grown in China during 2000-2018. The data simulation was based on calibrated AquaCrop modelling under furrow-, sprinkler-, and micro-irrigated as well as rainfed conditions. Data quality was validated by comparing the current results with multiple public datasets and remote-sensing products. The improved gridded WFCP dataset effectively compensated for the gaps in the existing datasets through: (i) revealing the intensity, structure, and spatiotemporal evolution of both productive and non-productive blue and green water consumption on a monthly scale, and (ii) including crop-by-crop unit WFCP benchmarks according to climatic zones.

## 1 Introduction

The grain production potential of irrigated agriculture can effectively cope with the pressure that population growth places on the food supply (Wada et al., 2013; Haddeland et al., 2014; Rosa et al., 2020; Puy et al., 2021; Wang et al., 2021) and restrain the encroachment of cultivated land on natural regions (Tilman et al., 2011; Brown and Pervez, 2014; Jägermeyr et al., 2017; Puy et al., 2020). Currently, irrigation accounts for more than 70% of worldwide blue water withdrawals (FAO, 2020) and 90% of global water consumption (Döll, 2009). Irrigated cropland increases the soil water content and releases water

30 vapour into the atmosphere, leading to an alteration in the hydrological cycle (Rodell et al., 2009; Elliott et al., 2014; Leng et  
31 al., 2014). Meanwhile, water scarcity is expected to increase in more than 80% of global farmlands, together with the  
32 increasingly serious threats on sufficient agricultural water supply by the competition for water among sectors (Yin et al., 2017;  
33 Pastor et al., 2019; Liu et al., 2022). Apparently, accurate assessment of water consumption on irrigated and rainfed farmlands  
34 is crucial for identifying water-use hotspots and ensuring a stable food supply, particularly in the context of climate change.

35 The consumptive water footprint of crop production (WFCP) measures the consumption of blue water (i.e., irrigation  
36 water extracted from surface and groundwater) and green water (i.e., soil water directly from rainfall) during the crop growth  
37 period (Hoekstra and Chapagain, 2008; Hoekstra et al., 2011; Hoekstra, 2013), permitting a unified evaluation of the water  
38 consumption of irrigated and rainfed crops (Lovarelli et al., 2016). The most widely used WFCP database is the WaterStat  
39 (Hoekstra and Mekonnen, 2012). It covers the WFCP of a wide variety of crops, crop derivatives, and biofuels, with data  
40 resolution at national, watershed, and county spatial scales, but it only contains 10-year averages for 1996-2005 (WFN, 2022).  
41 The CWASI database established by Tamea et al. (2021) fills the resultant gap concerning the interannual evolution of WFCP  
42 data through a fast-track approach (Tuninetti et al., 2017) at the national scale, suggesting that there is significant interannual  
43 variation in the water footprint per unit mass of crop production (uWFCP), which should be taken into account in analyses and  
44 applications. However, none of the aforementioned studies have considered intra-annual variations or intra-national differences  
45 in agricultural water consumption. Considering that disparities in space and time in the WFCP and uWFCP may have various  
46 effects on the formulation of water management measures. Such changes must be evaluated to provide a reference for seasonal  
47 water shortages (Hoekstra, 2013; Zhuo et al., 2016c).

48 Numerous studies have assessed the blue and green WFCP of specific crops at finer spatial and temporal resolutions using  
49 the agro-hydrological models including CROPWAT (Mekonnen and Hoekstra, 2011; Tuninetti et al., 2015), GEPIC (Liu et al.,  
50 2007), GCWM (Siebert and Döll, 2010), LPJmL (Fader et al., 2011), and AquaCrop (Zhuo et al., 2016b; Wang et al., 2019).  
51 Utilising the WATNEEDs model, Chiarelli et al. (2020) produced the first dataset to record global monthly blue and green  
52 water requirements of producing 23 crops at a 5 arcmin scale. They found that green water accounts for 84% of the considered  
53 global crop water requirements. However, the actual water consumption during crop production is frequently less than the  
54 predicted water requirement owing to soil water deficit, insufficient precipitation, and differences in field management (Long  
55 and Singh, 2013; Fisher et al., 2017). Furthermore, the aforementioned datasets ignore the non-negligible differences between  
56 the WFCP when using different water supply modes or irrigation practices and do not distinguish between the blue and green  
57 water consumption of two independent processes, namely soil evaporation (that is extravagant water consumption) and crop  
58 transpiration. In summary, the limitations of existing WFCP databases mean that they cannot be used to evaluate the effect of  
59 implementing water-saving irrigation practices on the spatiotemporal distribution of agricultural water consumption at a large

60 regional scale (Wang et al., 2019). Moreover, the lack of information on extravagant water consumption of crops in terms of  
61 the water sources and the spatiotemporal distribution hinders the precise implementation of water-saving agricultural policies  
62 and technologies (Jung et al., 2010; Lian et al., 2018).

63 To fill the abovementioned gaps in existing WFCP datasets, we developed a gridded dataset comprising monthly green  
64 and blue WFCP, evaporation and transpiration, and associated uWFCP benchmarks for 21 crops grown in China during 2000-  
65 2018. A self-sufficiency-oriented food policy has fuelled the explosive growth of water-saving irrigated farmlands in China in  
66 recent decades (SCIO, 1996; Ghose, 2014), with water-saving irrigated areas increasing by 5,698 kha from 2000 to 2018  
67 (representing 12% of the total irrigated area in 2018) (NBSC, 2022). The current study followed the WFN accounting  
68 framework (Hoekstra et al., 2011) and used FAO AquaCrop Plug-In program V6.0 to simulate the monthly WFCP at a  
69 resolution of 5 arcmin. The considered 21 crops account for 83% of national sown areas and 75% of national crop production  
70 in China (NBSC, 2022). The dataset differs from the others in four aspects: (i) It evaluated the effects of different water supply  
71 modes (irrigated or rain-fed) and irrigation practices (furrow, sprinkler, and micro-irrigation) on water consumption throughout  
72 the crop growth period. (ii) It distinguished between monthly blue and green water consumption via soil evaporation and crop  
73 transpiration. (iii) The dataset encompassed both the WFCP in  $\text{m}^3 \text{yr}^{-1}$  and the uWFCP in  $\text{m}^3 \text{ton}^{-1}$ . (iv) It identified uWFCP  
74 benchmarks that differentiated between various climatic zones and irrigation practices. The data quality was verified through  
75 its comparison with available public databases and remote sensing products.

## 76 **2 Data and methods**

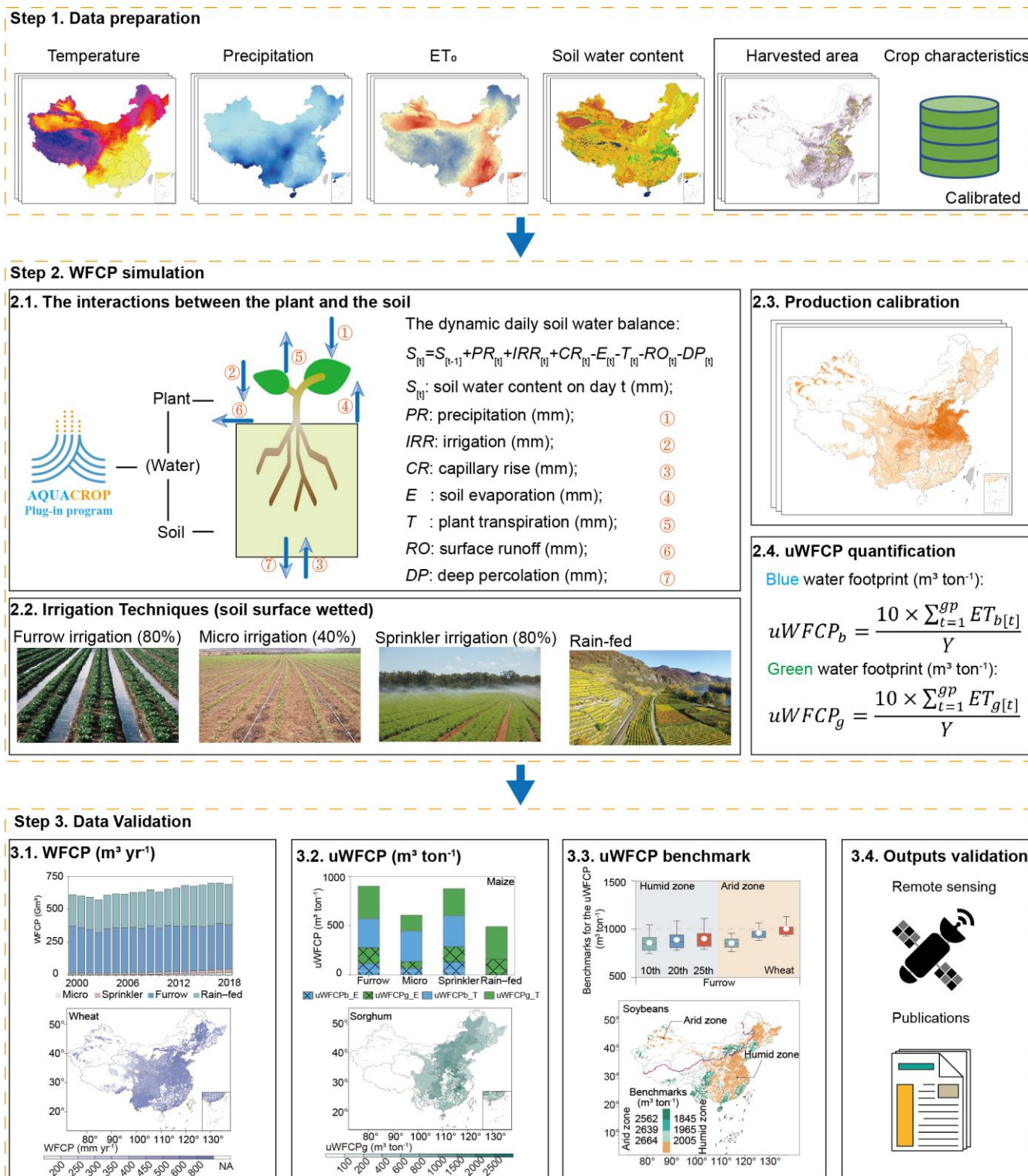
77 Three main steps were followed to create and validate the WFCP dataset under various water supply modes and irrigation  
78 practices during 2000-2018 (Fig. 1).

79 **Step 1: Data preparation.** We collected, verified, and inverted data on the yearly planting area of each crop under various  
80 water supply modes and irrigation practices at a resolution of 5 arcmin. The AquaCrop simulation required monthly  
81 precipitation, temperature, reference evapotranspiration ( $ET_0$ ), and  $\text{CO}_2$  datasets. The calibrated crop parameters were obtained  
82 from the published literature.

83 **Step 2: Water footprint simulation.** The AquaCrop model was run with daily steps to simulate soil evaporation, crop  
84 transpiration, and crop yield during the growth period of crops. The WFCP and uWFCP were calculated for different water  
85 supply modes and irrigation practices using a spatial resolution of 5 arcmin and a temporal resolution of months (Zhuo et al.,  
86 2016c; Wang et al., 2019).

87 **Step 3: Data validation.** The simulation results were verified by comparing them with remote sensing products of actual

88 evapotranspiration (Cheng et al., 2021) and publicly accessible WFCP datasets (Mekonnen and Hoekstra, 2011; Zhuo et al.,  
 89 2016a; Chiarelli et al., 2020).  
 90



91  
 92 **Figure 1. Three main steps for quantifying the water footprint of crop production.**

## 93 2.1 Data sources

### 94 2.1.1 Crop planting area and production

95 The irrigated and rain-fed areas of each crop from 2001 to 2018 were assigned at a resolution of 5 arcmin according to  
96 the base map for the year 2000 obtained from the MIRCA2000 dataset (Portmann et al., 2010) and interannual changes per  
97 province extracted from the China Statistical Yearbook (NBSC, 2022). At the provincial scale, irrigation data from 2000-2018  
98 were spatially divided into the proportional areas in which furrow, sprinkler, and micro-irrigation was used for each crop,  
99 retrieving data from the statistical yearbook (CAMIYC, 2022). Due to the lack of data in this regard, all vegetables were  
100 assumed to be grown under irrigation as based on agricultural practice. Further details about the planting area data selection  
101 have been provided in the Supplementary data and methods. The national production data for tomatoes and cabbage were  
102 derived from the Food and Agriculture Organization dataset (FAO, 2022) and was proportionally allocated to vegetable  
103 production by provinces. Production data for the remaining crops were obtained from the NBSC (2022).

### 104 2.1.2 Meteorological and soil data

105 The monthly data for precipitation, minimum and maximum temperature, and reference evapotranspiration were obtained  
106 from the Climatic Research Unit Time-Series 4.06 dataset (Harris et al., 2020). All meteorological data were resampled to a 5  
107 arcmin spatial resolution using the ArcGIS mapping platform. Atmospheric CO<sub>2</sub> concentration data were acquired from the  
108 Mauna Loa Observatory in Hawaii (Tans and Keeling, 2020). Soil texture data were obtained from the International Soil  
109 Reference and Information Centre (ISRIC) soil profile database (Dijkshoorn et al., 2008). Soil water content data were obtained  
110 from the ISRIC World Inventory of Soil Emission Potentials database (Batjes, 2012). Table 1 summarizes the data sources.

111

112 **Table 1. Inventory of data sources.**

Variables	Data source	Spatial resolution	Period	Data link
Irrigated and rainfed crop areas	MIRCA 2000	5 arcmin	2000-2018	<a href="https://www.uni-frankfurt.de/45218031/Data_download_center_for_MIRCA2000">https://www.uni-frankfurt.de/45218031/Data_download_center_for_MIRCA2000</a>
Crop production, yield and harvested areas	NBSC	Provincial	2000-2018	<a href="https://data.stats.gov.cn/adv.htm?m=advquery&amp;cn=E0103">https://data.stats.gov.cn/adv.htm?m=advquery&amp;cn=E0103</a>
Production of vegetables	FAOSTAT	National	2000-2018	<a href="https://www.fao.org/faostat/en/#data/QV">https://www.fao.org/faostat/en/#data/QV</a>
Area of different irrigation techniques	CAMIY	Provincial	2000-2018	<a href="https://data.cnki.net/Trade/yearbook/single/N2021040192?zcode=Z032">https://data.cnki.net/Trade/yearbook/single/N2021040192?zcode=Z032</a>
Meteorological data	CRU TS v. 4.03	30 arcmin	2000-2018	<a href="https://crudata.uea.ac.uk/cru/data/hrg/">https://crudata.uea.ac.uk/cru/data/hrg/</a>

CO <sub>2</sub> concentration	NOAA	Average	2000-2018	<a href="https://gml.noaa.gov/ccgg/trends/data.html">https://gml.noaa.gov/ccgg/trends/data.html</a>
Soil texture	ISRIC	1 arcmin	-	<a href="https://data.isric.org/geonetwork/srv/eng/catalog.search#/metadata/2919b1e3-6a79-4162-9d3a-e640a1dc5aef">https://data.isric.org/geonetwork/srv/eng/catalog.search#/metadata/2919b1e3-6a79-4162-9d3a-e640a1dc5aef</a>
Initial soil moisture content	ISRIC	5 arcmin	-	<a href="https://data.isric.org/geonetwork/srv/eng/catalog.search#/metadata/82f3d6b0-a045-4fe2-b960-6d05bc1f37c0">https://data.isric.org/geonetwork/srv/eng/catalog.search#/metadata/82f3d6b0-a045-4fe2-b960-6d05bc1f37c0</a>

113 Note: “-” means constant values.

114

### 115 2.1.3 Crop characteristics

116 The characteristics of crops selected for this study are listed in Table 2. Due to differences in their phenology, wheat,  
 117 maize, barley, and rapeseed had two sowing periods, whereas rice had three sowing periods across the study’s time frame. The  
 118 growth period of all crops was divided into four stages based on their growth characteristics (Allen et al., 1998; Vanuytrecht  
 119 et al., 2014): the initial (L1), crop development (L2), mid-season (L3), and late-season (L4) growth stages. Crop planting dates  
 120 were retrieved from Chen et al. (1995). The phenology selection procedure is delineated and the sensitivity analysis of WFCP  
 121 to phenology are performed within the phenology selection of Supplementary data and methods. The reference harvest index  
 122 (HI<sub>0</sub>) from Xie et al. (2011) and Zhang and Zhu (1990), and crop growth stages and maximum root depth from Allen et al.  
 123 (1998) and Hoekstra and Chapagain (2006).

124

125 **Table 2. Crop characteristics for the 21 crops in China.**

Crop class	Crop code	Planting date	Length of crop development stage (day)				Root deeps (m)		WP*	HI <sub>0</sub>
			L1	L2	L3	L4	Irrigated	Rainfed		
Wheat	1									
Spring wheat		15th Mar	20	25	60	30	1	1.5	15	39
Winter wheat		15th Oct	30	140	40	30	1.5	1.8	15	40
Maize	2									
Spring maize		15th Apr	30	40	50	30	1	1.7	33.7	44
Summer maize		1st Jun	20	35	40	30	1	1.7	33.7	43
Rice	3									
Early rice		15th Mar	30	30	30	30	0.5		19	44
Mid rice		15th Apr	30	30	60	30	0.5		19	44
Late rice		15th Jul	30	30	70	40	0.5		19	44
Sorghum	4	1st May	20	35	45	30	1	2	33.7	39
Millet	5	15th Apr	15	55	40	20	1	1.5	32	47
Barley	6									
Spring barley		15th Apr	15	35	50	30	1	1.5	15	39
Winter barley		25th Oct	20	110	40	35	1	1.5	15	39

Soybeans	7	1st Jun	20	40	60	30	0.6	1.3	15	44
Potatoes	8	1st May	25	30	45	30	0.4	0.6	18	69
Sweet potatoes	9	1st May	20	30	60	40	1	1.5	18	59
Cotton	10	1st Apr	30	50	55	45	1	1.7	15	38
Sugar cane	11	1st Feb	30	50	180	60	1.2	2	30	60
Sugar beets	12	15th Apr	50	40	50	40	0.7	1	17	71
Groundnuts	13	15th Apr	10	80	35	25	0.5	1	17	43
Rapeseed	14									
Spring rapeseed		15th Apr	6	69	20	36	0.8	1.5	17	32
Winter rapeseed		30th Sep	6	148	20	36	0.8	1.5	17	32
Sunflower	15	15th Apr	25	35	45	25	0.8	1.5	18	31
Tomatoes	16	15th Jan	30	40	40	25	0.7	1.5	18	40
Apple	17	1st Mar	30	50	130	30	1	2	20	20
Tea	18	15th Feb	120	60	180	5	0.9	0.9	17	5
Tobacco	19	15th May	20	30	30	30	0.8	0.8	17	61
Cabbage	20	5th Jul	40	60	50	15	0.5	0.8	15	67
Grapes	21	1st Apr	30	60	40	80	1		17	2

126

## 127 2.2 Methods

### 128 2.2.1 Spin-up for the model

129 To establish the initial soil moisture content at the beginning of the growing season, the method and assumptions proposed  
130 by Siebert and Döll (2010) were adopted. Following their approach, the initial soil moisture content was generated utilizing  
131 the maximum soil moisture content of rainfed fallow land in the two years preceding the planting period. The initial soil  
132 moisture at the start of the growing period is assumed as green water. Such settings and assumptions have been extensively  
133 applied and with acceptable uncertainties (Chiarelli et al., 2020; Hoogeveen et al., 2015).

### 134 2.2.2 Parameterization of perennial crop

135 In AquaCrop, the simulated annual crops are programmed to die at the harvest stage, signifying the completion of their  
136 life cycle, upon which their biomass is reduced to zero. This stands in contrast to perennial plants such as tea and apple trees,  
137 where the harvest of fruits does not result in the complete loss of the standing biomass. To accommodate the simulation of  
138 perennial crops in AquaCrop, the model is used differently than the normal model set-up. We attempted to simulate the  
139 perennial crops by simulating the foliage, twigs and stem of the plants following Poppe (2016). These components are  
140 considered the annual portion of perennial crops within the scope of this study. The remaining biomass, including major  
141 branches, is assumed to remain constant once the tree matures. Additionally, there will also be no root development for the

142 crop. Since yield is a direct function of biomass and harvest index, adjustments are made to the harvest index to reflect its  
 143 applicability to foliage, twigs and stem biomass, rather than the whole biomass. Similar to other crops, the evapotranspiration  
 144 of perennial crops is directly associated with the canopy cover.

### 145 2.2.3 Calculation of uWFCP

146 The blue and green uWFCP were obtained from the blue and green components of the WFCP (evapotranspiration during  
 147 the crop growth period) in relation to the crop yield (Hoekstra et al., 2011).

$$148 \quad uWFCP_b = \frac{10 \times \sum_{t=1}^{gp} ET_{b[t]}}{Y} \quad (1)$$

$$149 \quad uWFCP_g = \frac{10 \times \sum_{t=1}^{gp} ET_{g[t]}}{Y} \quad (2)$$

150 where  $uWFCP_b$  and  $uWFCP_g$  are the blue and green uWFCP, respectively ( $m^3 \text{ ton}^{-1}$ );  $ET_b$  and  $ET_g$  are the blue and green WFCP  
 151 (that is,  $WFCP_b$  and  $WFCP_g$ ), respectively (mm) (see equations 8 and 9);  $gp$  represents the days in the growing period; 10 is  
 152 the unit conversion factor;  $Y$  (see equation 4 below) is the crop yield ( $\text{ton ha}^{-1}$ ); and  $t$  indicates a given day.

153 The daily aboveground biomass production ( $B$ ) was obtained as follows:

$$154 \quad B = WP^* \times \sum \frac{Tr_{[t]}}{ET_{0[t]}} \quad (3)$$

155 where  $WP^*$  ( $\text{ton ha}^{-1}$ ) expresses the aboveground dry matter produced per unit land area per unit of transpired water, which is  
 156 governed by a combination of atmospheric  $CO_2$  concentration, crop type (C3 and C4 crops), and soil fertility. The  $WP^*$  is  
 157 multiplied with the ratio of crop transpiration ( $Tr$ ) to the reference evapotranspiration ( $ET_0$ ) for that day. The goal of  
 158 normalisation is to make  $WP^*$  applicable to diverse locations and seasons, including future climate scenarios.

159 The crop yield ( $Y$ ) ( $\text{ton ha}^{-1}$ ) was obtained by multiplying the aboveground biomass ( $B$ ) with an adjusted reference harvest  
 160 index:

$$161 \quad Y = f_{HI} HI_0 B \quad (4)$$

162 where  $f_{HI}$  is the calibration coefficient of the standardised harvest index  $HI_0$ , which is influenced by water stress and  
 163 temperature stress.

### 164 2.2.4 Dynamic daily soil water balance

165 By tracking the daily incoming and outgoing water fluxes at the root zone boundary, the dynamic daily soil water balance  
 166 was calculated as follows (Mekonnen and Hoekstra, 2010):

$$167 \quad S_{[t]} = S_{[t-1]} + PR_{[t]} + IRR_{[t]} + CR_{[t]} - ET_{[t]} - RO_{[t]} - DP_{[t]} \quad (5)$$

168 where  $S$  is the soil water content (mm);  $PR$  is the precipitation (mm);  $IRR$  is the irrigation water volume (mm);  $CR$  is the



169 capillary rise from groundwater, assumed to be zero (mm); RO is the surface runoff (mm); DP is the deep soil percolation  
 170 (mm); and ET is the actual evapotranspiration (mm), consisting of soil evaporation ( $E$ ) and crop transpiration (Tr), which were  
 171 calculated as follows:

$$172 \quad E = (K_r K_e) ET_0 \quad (6)$$

$$173 \quad Tr = (K_s K_{S_{Tr}} K_{C_{Tr}}) ET_0 \quad (7)$$

174 where  $K_r$  is the evaporation reduction coefficient, which is less than 1 (dimensionless);  $K_e$  is the soil evaporation coefficient,  
 175 which is proportional to the fraction of the soil surface not covered by the canopy (dimensionless);  $K_s$  is the soil water stress  
 176 coefficient, which is smaller than 1 when there is insufficient soil water to meet the evaporative demand of the atmosphere  
 177 (dimensionless);  $K_{S_{Tr}}$  is the cold stress coefficient, which drops below 1 when the temperature is insufficient for growth  
 178 (dimensionless); and  $K_{C_{Tr}}$  is the crop transpiration coefficient, which is proportional to the green canopy cover  
 179 (dimensionless).

180 By tracking the proportional contribution of daily rainfall and irrigation water to each element of the soil water balance,  
 181  $ET_{b[t]}$ ,  $ET_{g[t]}$ ,  $E_{b[t]}$ ,  $E_{g[t]}$ ,  $Tr_{b[t]}$  and  $Tr_{g[t]}$  were extracted (Zhuo et al., 2016c; Chukalla et al., 2015):

$$182 \quad ET_{b[t]} = IRR_{[t]} + S_{b[t-1]} - S_{b[t]} - RO_{[t]} \left( \frac{IRR_{[t]}}{PR_{[t]} + IRR_{[t]}} \right) - DP_{[t]} \left( \frac{S_{b[t-1]}}{S_{[t-1]}} \right) \quad (8)$$

$$183 \quad ET_{g[t]} = PR_{[t]} + S_{g[t-1]} - S_{g[t]} - RO_{[t]} \left( \frac{PR_{[t]}}{PR_{[t]} + IRR_{[t]}} \right) - DP_{[t]} \left( \frac{S_{g[t-1]}}{S_{[t-1]}} \right) \quad (9)$$

$$184 \quad E_{b[t]} = E_{[t]} \left( \frac{S_{b[t-1]}}{S_{[t-1]}} \right) \quad (10)$$

$$185 \quad E_{g[t]} = E_{[t]} \left( \frac{S_{g[t-1]}}{S_{[t-1]}} \right) \quad (11)$$

$$186 \quad Tr_{b[t]} = Tr_{[t]} \left( \frac{S_{b[t-1]}}{S_{[t-1]}} \right) \quad (12)$$

$$187 \quad Tr_{g[t]} = Tr_{[t]} \left( \frac{S_{g[t-1]}}{S_{[t-1]}} \right) \quad (13)$$

188 where  $S_{b[t]}$  and  $S_{g[t]}$  are the blue and green soil water content (mm) for a crop, respectively, at the end of day  $t$ . Following Zhuo  
 189 et al. (2016c), the green water value was used as the initial soil water content in each calculation cell.

## 190 2.2.5 Irrigation practices module

191 Different irrigation practices indirectly affect water consumption during the growth period due to differences in the  
 192 fraction of the surface wetted ( $f_w$ ) by each method (Raes et al., 2018). The soil evaporation coefficient ( $K_e$ ) was multiplied by  
 193 the  $f_w$ -value to account for partial wetness when only a portion of any soil surface was irrigated. This irrigation practices  
 194 differentiation approach is commonly used before (Pereira et al., 2015; Wang et al., 2019; Chibarabada et al., 2020; Li et al.,  
 195 2022; Yue et al., 2022). We employed a supplementary irrigation strategy whereby irrigation is applied when soil moisture

196 falls below the plant wilting point to bring it up to field capacity. Owing to special environmental restrictions, furrow irrigation  
 197 was used for rice planting in this study. Specific irrigation conditions were divided into either sufficient or water-demanding  
 198 subtypes (irrigation to field capacity when the soil water content reached the wilting point).

$$199 \quad K_e = f_w(1 - CC^*)K_{ex} \quad (14)$$

$$200 \quad (1 - CC^*) = 1 - 1.72CC + CC^2 - 0.3CC^3 \quad \geq 0 \quad (15)$$

201 where the  $f_w$ -values used for furrow, sprinkler, and micro-irrigation were 80%, 100%, and 40%, respectively;  $(1 - CC^*)$  is the  
 202 dimensionless adjusted fraction of the non-covered soil surface (dimensionless);  $CC$  is canopy cover ( $m^2 m^{-2}$ ); and  $K_{ex}$   
 203 is the maximum soil evaporation coefficient (dimensionless) for fully wet and non-shaded soil surfaces.

## 204 **2.2.6 Benchmarks for uWFCP**

205 In contrast to variables such as rain-fed and irrigated croplands, wet and dry years, warm and cold years, different soil  
 206 types, climate zone was evidenced to be the key factor influencing regional uWFCP benchmarks (Zhuo et al., 2016b). Therefore,  
 207 we classified China's climatic regions based on the aridity index (Middleton and Thomas, 1997) (AI; defined as the ratio of  
 208 rainfall to reference evapotranspiration) and set up regional uWFCP benchmarks for humid ( $AI > 0.5$ ) and arid ( $AI < 0.5$ )  
 209 zones. The uWFCP of each grid in the same climate zone was ranked from lowest to highest, and the uWFCP corresponding  
 210 to a cumulative crop production of 10%, 20% and 25% of the total production were recorded as the regional uWFCP  
 211 benchmarks (Mekonnen and Hoekstra, 2014; Zhuo et al., 2016b; Wang et al., 2019; Yue et al., 2022).

## 212 **2.3 Calibration and validation**

### 213 **2.3.1 Production calibration**

214 Given the data accessibility, the current study utilized provincial statistics to validate the simulated production by scaling  
 215 each grid-based simulated result using provincial calibration coefficients ( $R$ ), rather than forcing the simulated production of  
 216 all grid within a province to a constant value (Mialyk et al., 2022; Yue et al., 2022; Zhuo et al., 2016a). This approach  
 217 maintained the spatial variability of simulated production within each province.

$$218 \quad R = \frac{P\_P_{sta}}{\sum_{i=1}^4 P\_G_{i,sim}} \quad (16)$$

$$219 \quad P\_G_{i,act} = P\_G_{i,sim} \cdot R \quad (17)$$

220 where  $P\_P_{NBSC}$  is the statistical (sta) provincial crop production ( $ton yr^{-1}$ );  $i$  represents the water supply modes and irrigation  
 221 practices;  $P\_G_{i,sim}$  is the simulated (sim) grid crop production value ( $ton yr^{-1}$ ) according to  $i$ ; and  $P\_G_{i,act}$  is the actual (act) grid  
 222 crop production value ( $ton yr^{-1}$ ) according to  $i$ .

223 It should be noted that although provincial yearbooks include some city-level crop production data, considering the  
224 numerous crop types involved in this study, and the division of certain crops by harvest periods (e.g. winter wheat, spring  
225 wheat, early rice, mid rice, late rice), there are indeed many instances of missing and incomplete data at the city scale. The  
226 meteorological and soil factors are critical factors affecting the estimation of WFCP (Zhuo et al., 2014; Tuninetti et al., 2015).  
227 Consequently, the simulated outcomes can exhibit spatial heterogeneity after integrating high-resolution soil texture,  
228 precipitation, temperature, and other model inputs, even with provincial production calibration.

### 229 **2.3.2 Remote sensing validation**

230 Because of the spatially fragmented nature of crop cultivation, the water consumption results of current study were  
231 validated against the dual-source (PML-V2(China)) and single-source (SEBAL) remote sensing products over screened grids  
232 to reduce the interference of non-agricultural land with the validation results. According to Chinese Agricultural Cropping  
233 System (IGSNRR, 2022), we selected grids in which the sum of planted areas was greater than 5 kha (> 50% of a single grid)  
234 and greater than 10 kha (>100% of a single grid) for single- and multi-crop regions, respectively. In terms of the time span, 19  
235 of the 21 crops studied experienced growth periods from April to August; therefore, these five months were set as the validation  
236 interval in terms of total evapotranspiration. The PML-V2 (He et al., 2022) and SEBAL (Cheng et al., 2021) products had  
237 spatial resolutions of 500 m and 1 km, respectively, with a temporal resolution of 1 day. Bilinear was implemented to resample  
238 the data to 5 arc-min. Notably, the SEBAL products solely comprised aggregate evapotranspiration figures, whereas the PML-  
239 V2 separated land surface evapotranspiration into vegetation transpiration ( $E_c$ ), soil evaporation ( $E_s$ ), evaporation of  
240 intercepted precipitation ( $E_i$ ), and water body evaporation ( $E_w$ ). In this study,  $E_c + E_s$ ,  $E_c$  and  $E_s$  were compared with the  
241 generated ET, E and T data, respectively.

### 242 **2.3.3 Publications comparison**

243 The present dataset was compared with published studies that included temporal and spatial data overlaps. The  
244 comparison included the crop planting area at the grid scale (IFPRI, 2019; Grogan et al., 2022), and the WFCP and uWFCP  
245 values at the grid and national scale (Mekonnen and Hoekstra, 2011; Zhuo et al., 2016a; Chiarelli et al., 2020; Cheng et al.,  
246 2021).

### 247 **2.3.4 Accuracy assessment**

248 The linear regression coefficient ( $R^2$ ) was used to measure the consistency between the statistical data, remote sensing  
249 data, and simulated results. The Root Mean Square Error ( $RMSE$ ) metric was utilized to evaluate model performance.

250 Mathematically, the  $R^2$  and  $RMSE$  can be expressed as:

$$251 \quad R^2 = \frac{(\sum_{i=1}^n (x_i - \bar{x}_i) \times (\text{ref}_i - \overline{\text{ref}_i}))^2}{\sum_{i=1}^n (x_i - \bar{x}_i)^2 \times \sum_{i=1}^n (\text{ref}_i - \overline{\text{ref}_i})^2} \quad (18)$$

$$252 \quad RMSE = \sqrt{\frac{1}{n} \sum_{i=1}^n (x_i - \text{ref}_i)^2} \quad (19)$$

253 where  $n$  indicate the number of samples;  $x_i$  and  $\text{ref}_i$  represent the simulated and statistical values (remote sensing data),  
 254 respectively;  $\bar{x}_i$  and  $\overline{\text{ref}_i}$  are the mean values of the simulated and statistical values (remote sensing data), respectively.

## 255 Results

### 256 3.1 Water footprint of crop production

257 During the study period, the WFCP of 21 crops in China increased by 13% to 690 Gm<sup>3</sup> yr<sup>-1</sup> in 2018, with WFCP<sub>b</sub> and  
 258 WFCP<sub>g</sub> accounting for 29% and 71% of this increase, respectively. The WFCP<sub>b</sub> and WFCP<sub>g</sub> varied greatly across crops, time,  
 259 and space. Table 3 presents the WFCP of the 21 crops under different water supply modes and irrigation practices in 2018.  
 260 Maize (165 Gm<sup>3</sup> yr<sup>-1</sup>), rice (143 Gm<sup>3</sup> yr<sup>-1</sup>), and wheat (125 Gm<sup>3</sup> yr<sup>-1</sup>) had the highest annual average WFCP, accounting for  
 261 67% of the total WFCP. The WFCP of grapes (177%) and maize (94 Gm<sup>3</sup> yr<sup>-1</sup>) showed the greatest growth rate, with their  
 262 planting areas expanding by 156% and 82%, respectively (NBSC, 2022).

263

264 **Table 3. WFCP and planting area under different water supply modes and irrigation practices for 21 crops in 2018.**

Crop	Furrow irrigation			Micro irrigation			Sprinkler irrigation			Rain-fed	
	WFCP <sub>b</sub>	WFCP <sub>g</sub>	Area	WFCP <sub>b</sub>	WFCP <sub>g</sub>	Area	WFCP <sub>b</sub>	WFCP <sub>g</sub>	Area	WFCP <sub>g</sub>	Area
	M m <sup>3</sup>	M m <sup>3</sup>	k ha	M m <sup>3</sup>	M m <sup>3</sup>	k ha	M m <sup>3</sup>	M m <sup>3</sup>	k ha	M m <sup>3</sup>	k ha
	(△)	(△)	(△)	(△)	(△)	(△)	(△)	(△)	(△)	(△)	(△)
Wheat	40,595	35,702	13,157	4,384	2,369	1,357	2,170	1,583	625	41,046	9,127
	(-22%)	(-9%)	(-18%)	(1936%)	(1650%)	(1964%)	(-26%)	(-10%)	(-20%)	(5%)	(-6%)
Maize	31,023	40,092	13,122	5,581	3,604	1,611	4,351	4,413	1,538	120,279	25,859
	(3%)	(18%)	(12%)	(4577%)	(2950%)	(3413%)	(67%)	(107%)	(95%)	(162%)	(147%)
Rice	81,847	58,979	28,306	-	-	-	4,629	5,540	1,883	-	-
	(4%)	(1%)	(-4%)	-	-	-	(329%)	(404%)	(366%)	-	-
Sorghum	346	457	157	57	46	21	53	53	20	1,757	424
	(-36%)	(-20%)	(-27%)	(3124%)	(2259%)	(2583%)	(34%)	(85%)	(66%)	(-35%)	(-36%)
Millet	346	388	137	43	32	16	46	42	16	2,652	609
	(-27%)	(-10%)	(-20%)	(2176%)	(1786%)	(2032%)	(10%)	(41%)	(28%)	(-38%)	(-43%)
Barley	91	133	67	14	12	7	6	7	3	768	235
	(-48%)	(-48%)	(-52%)	(4024%)	(3355%)	(2902%)	(-3%)	(3%)	(-13%)	(-67%)	(-65%)
Soybeans	3,936	6,751	1,963	413	375	144	389	609	193	27,319	6,113
	(-22%)	(-16%)	(-19%)	(2315%)	(1871%)	(2031%)	(35%)	(102%)	(88%)	(-7%)	(-10%)
Potatoes	721	966	377	140	78	39	91	88	34	16,171	4,440
	(-20%)	(11%)	(14%)	(3694%)	(2962%)	(3256%)	(50%)	(121%)	(106%)	(8%)	(1%)
Sweet potatoes	873	1,653	427	37	57	16	37	59	16	10,276	1,921
	(-64%)	(-55%)	(-57%)	(429%)	(561%)	(513%)	(-67%)	(-44%)	(-51%)	(-60%)	(-60%)
Cotton	2,195	2,268	625	788	217	134	85	82	23	9,824	2,573
	(-54%)	(-45%)	(-52%)	(4353%)	(1770%)	(3006%)	(-59%)	(-37%)	(-49%)	(-27%)	(-5%)
Sugar cane	258	589	98	9	20	3	8	17	3	10,924	1,302

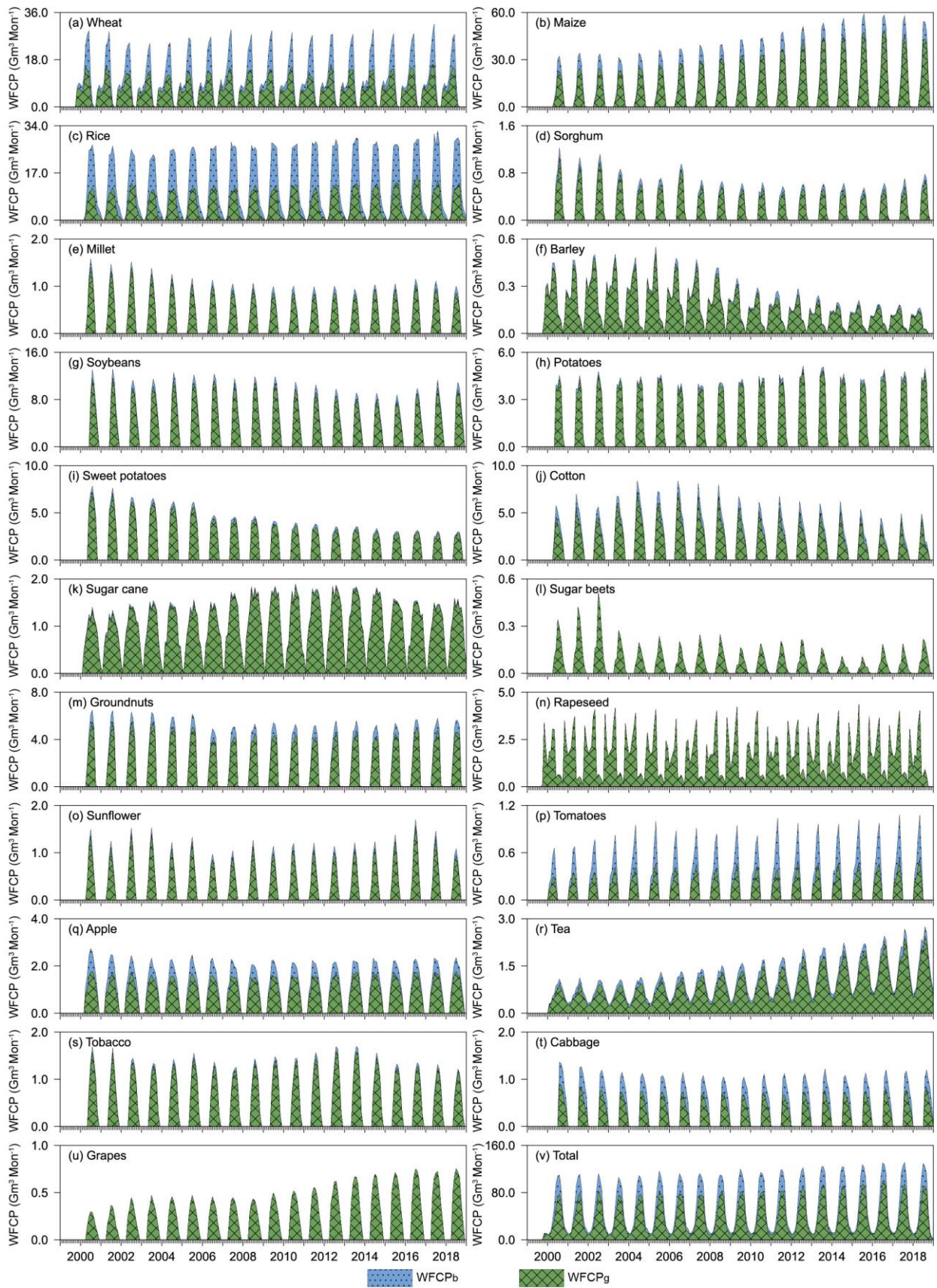
	(-36%)	(-37%)	(-40%)	(1309%)	(1196%)	(1145%)	(163%)	(170%)	(150%)	(32%)	(28%)
Sugar beets	0.096	0.029	0.021	0.145	0.043	0.056	0.003	0.001	0.002	812	216
	(-78%)	(-78%)	(-72%)	(5530%)	(5859%)	(12331%)	(-85%)	(-85%)	(-61%)	(-34%)	(-34%)
Groundnuts	3,500	4,842	1,435	209	178	66	210	223	72	14,441	3,046
	(-6%)	(4%)	(-3%)	(1776%)	(1596%)	(1587%)	(11%)	(62%)	(42%)	(-6%)	(-8%)
Rapeseed	0.0159	0.0539	0.0147	0.0001	0.0002	0.0001	0.0001	0.0005	0.0001	19,053	6,551
	(256%)	(37%)	(67%)	(3336%)	(1653%)	(1800%)	(2660%)	(965%)	(1194%)	(3%)	(-13%)
Sunflower	262	202	87	137	49	33	34	21	10	2,913	792
	(-35%)	(-16%)	(-26%)	(8591%)	(5601%)	(6626%)	(-1%)	(22%)	(10%)	(-25%)	(-28%)
Tomatoes	1,365	1,581	949	74	57	44	74	69	47	-	-
	(48%)	(60%)	(45%)	(2379%)	(2463%)	(2270%)	(109%)	(198%)	(144%)	-	-
Apple	2,366	2,223	568	352	226	85	166	134	36	7,551	1,250
	(-47%)	(-32%)	(-41%)	(1638%)	(1236%)	(1452%)	(-53%)	(-37%)	(-44%)	(11%)	(2%)
Tea	2,218	3,200	550	51	86	15	68	92	16	13,803	1,730
	(65%)	(46%)	(43%)	(1690%)	(1622%)	(1464%)	(427%)	(453%)	(404%)	(242%)	(252%)
Tobacco	308	673	201	13	39	12	14	26	8	3,819	836
	(-30%)	(-12%)	(-18%)	(1181%)	(1800%)	(1848%)	(-34%)	(21%)	(4%)	(-28%)	(-29%)
Cabbage	1,523	2,642	897	72	96	42	76	124	45	-	-
	(-18%)	(-19%)	(-24%)	(1183%)	(1033%)	(1136%)	(15%)	(47%)	(28%)	-	-
Grapes	0.013	0.006	0.003	0.033	0.015	0.008	0.0004	0.0002	0.0001	3,869	725
	(-58%)	(-59%)	(-58%)	(17901%)	(17826%)	(18248%)	(-71%)	(-71%)	(-71%)	(177%)	(156%)

265 Note: “△” refers to the rate of change from 2000 to 2018. “-” indicates that no crops are grown.

266

267 In addition, the annual average proportions of WFCP attributable to furrow irrigation and rain-fed conditions reached 53%  
268 and 44%, respectively (Fig. S1). Nevertheless, the WFCP of sprinkler and micro-irrigation expanded by 11 and 19 Gm<sup>3</sup> yr<sup>-1</sup>,  
269 respectively, increasing their proportional contribution to the total WFCP by respective factors of 1.6 and 23. Over the same  
270 period, WFCP under furrow irrigation decreased by 5%. Considering the positive correlation between WFCP and the cultivated  
271 area under different water supply and irrigation practices, the above results reflect that sprinkler and micro-irrigation planting  
272 modes are being deployed more often on existing and freshly reclaimed farmland in China (NBSC, 2022). Given the large  
273 scale of crop cultivation in China, such a significant shift in irrigation practices will have important implications: (i) it will  
274 affect the quantification of national crop water consumption; (ii) it will create market opportunities while concurrently  
275 propelling technological innovation in the irrigation infrastructure. In conclusion, when quantifying and evaluating the WFCP,  
276 it is vital to consider the influence of various water supply modes and irrigation practices (Wang et al., 2019).

277



278

279 **Figure 2. Total national monthly WFCP<sub>g</sub> and WFCP<sub>b</sub> of 21 crops in China over 2000-2018.**

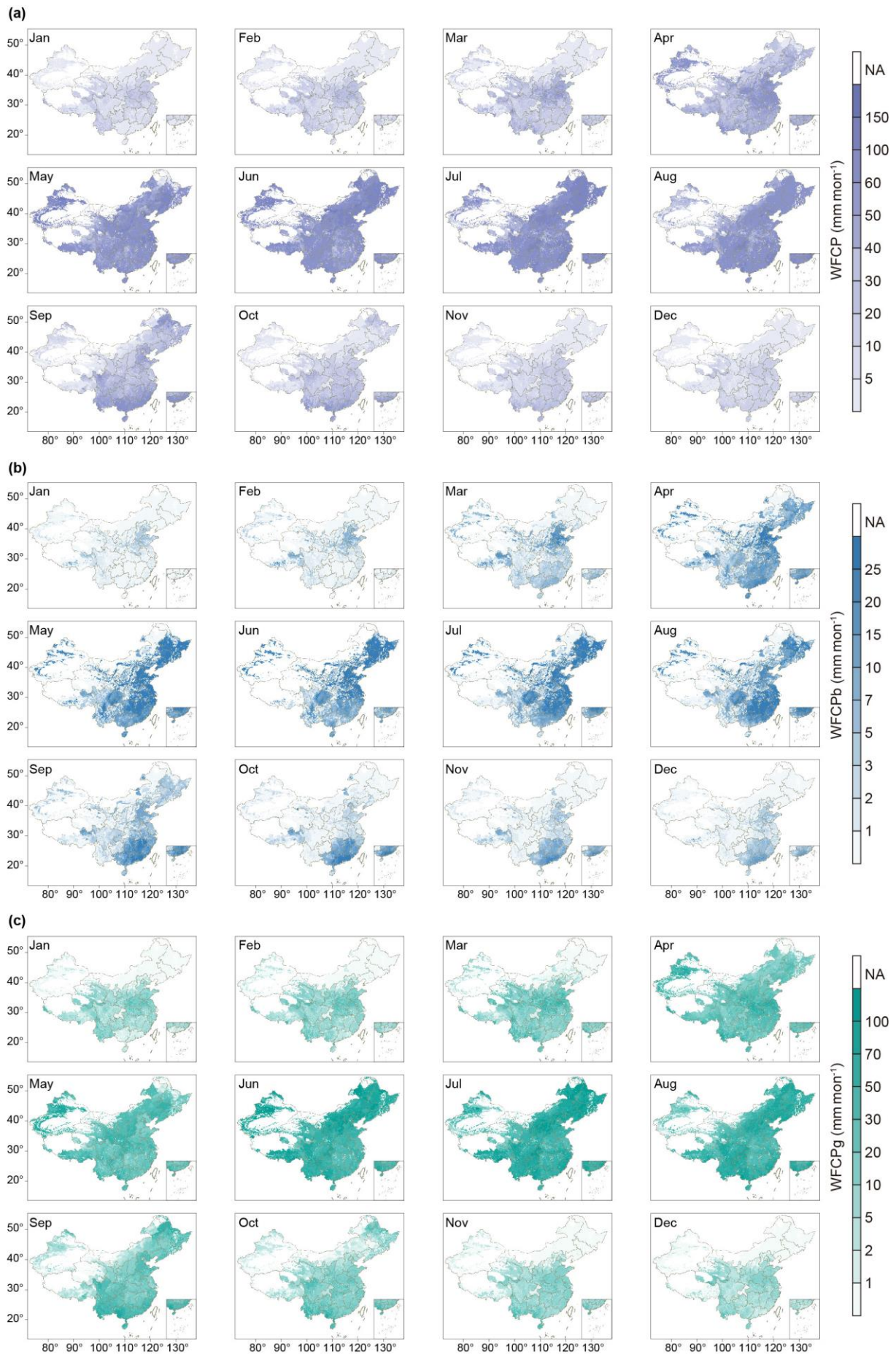
280

281 The water source accessed for crop production varied cyclically across years (Fig. 2). The WFCP<sub>b</sub> peaked annually in

282 May, with an average annual value of  $16 \text{ Gm}^3 \text{ mon}^{-1}$ ; water usage by rice and maize crops were responsible for 40% and 37%  
283 of this value, respectively. In January and February of each year, the  $\text{WFCP}_g$  comprised almost 75% of the monthly WFCP.  
284 The annual peak of the  $\text{WFCP}_g$  alternated between June and July, with an average annual value of  $83 \text{ Gm}^3 \text{ mon}^{-1}$ , 40% of which  
285 was attributable to water consumption by maize crops. The monthly WFCP values revealed that the peaks of evaporation  
286 (average annual value of  $45 \text{ Gm}^3 \text{ mon}^{-1}$ ) and transpiration (average annual value of  $56 \text{ Gm}^3 \text{ mon}^{-1}$ ) for the 21 crops occurred  
287 in May and July, respectively (Fig. S2 and S3). The monthly WFCP fluctuated within each crop; nevertheless, the relative  
288 contributions of evapotranspiration and transpiration to total water consumption during the same growth period varied less  
289 from year to year. The above analysis allowed us to identify the quantity, type, and periods of water consumption by each crop.

290 The grid-scale spatial distributions of the monthly WFCP,  $\text{WFCP}_b$ , and  $\text{WFCP}_g$  values are shown in Fig. 3. The months  
291 with large grid WFCP ( $\text{WFCP} > 50 \text{ mm mon}^{-1}$ ,  $\text{WFCP}_b > 10 \text{ mm mon}^{-1}$ , and  $\text{WFCP}_g > 30 \text{ mm mon}^{-1}$ ) mainly comprised April  
292 to August. The Northeast Plain, North Plain, and Sichuan Basin contained the regions with the highest grid WFCP. The grid  
293 WFCP varied considerably among the 21 crops, but its spatial distribution was consistent within the planted area of each crop.  
294 In addition, the regional distribution of grid  $\text{WFCP}_b$  and  $\text{WFCP}_g$  values of each crop exhibited significant spatial heterogeneity  
295 (Fig. S4 and S5). The grid WFCP,  $\text{WFCP}_b$ , and  $\text{WFCP}_g$  of sprinkler irrigation at the monthly and annual scales were  
296 significantly higher than those of the other two irrigation practices, and high-value regions were concentrated in the northeast,  
297 southwest, and south of China (Fig. S6–S10). This is attributable to the substantially higher surface wetting fraction achieved  
298 with sprinkler irrigation relative to furrow and micro irrigation, which augments crop water consumption per unit cultivated  
299 area during the growing period by affecting soil evaporation coefficient (Equations 6, 7 and 14). The relative blue and green  
300 water consumption via evaporation and transpiration depended on the natural conditions prevailing at the time and in the space  
301 where the 21 crops were grown, as well as the water supply modes and irrigation practices (Fig. S11–S14).

302



303

304

Figure 3. Gridded monthly total WFCP (a), WFCPb (b), and WFCPg (c) of 21 crops in China by 2017.



### 3.2 Water footprint per unit of crop production

306

Tea ( $8372 \text{ m}^3 \text{ ton}^{-1}$ ), cotton ( $3974 \text{ m}^3 \text{ ton}^{-1}$ ), and tobacco ( $2242 \text{ m}^3 \text{ ton}^{-1}$ ) had comparatively large uWFCP, whereas fruits

307

and vegetables had a uWFCP of less than  $500 \text{ m}^3 \text{ ton}^{-1}$ . Among the grain crops, wheat and maize had uWFCP of  $1110 \text{ m}^3 \text{ ton}^{-1}$

308

and  $883 \text{ m}^3 \text{ ton}^{-1}$ , respectively. Late rice ( $826 \text{ m}^3 \text{ ton}^{-1}$ ) had a slightly greater uWFCP than early ( $654 \text{ m}^3 \text{ ton}^{-1}$ ) and mid ( $732$

309

$\text{m}^3 \text{ ton}^{-1}$ ) rice. The uWFCP, uWFCP<sub>b</sub>, and uWFCP<sub>g</sub> for all 21 crops showed a trend of fluctuating decline during the study

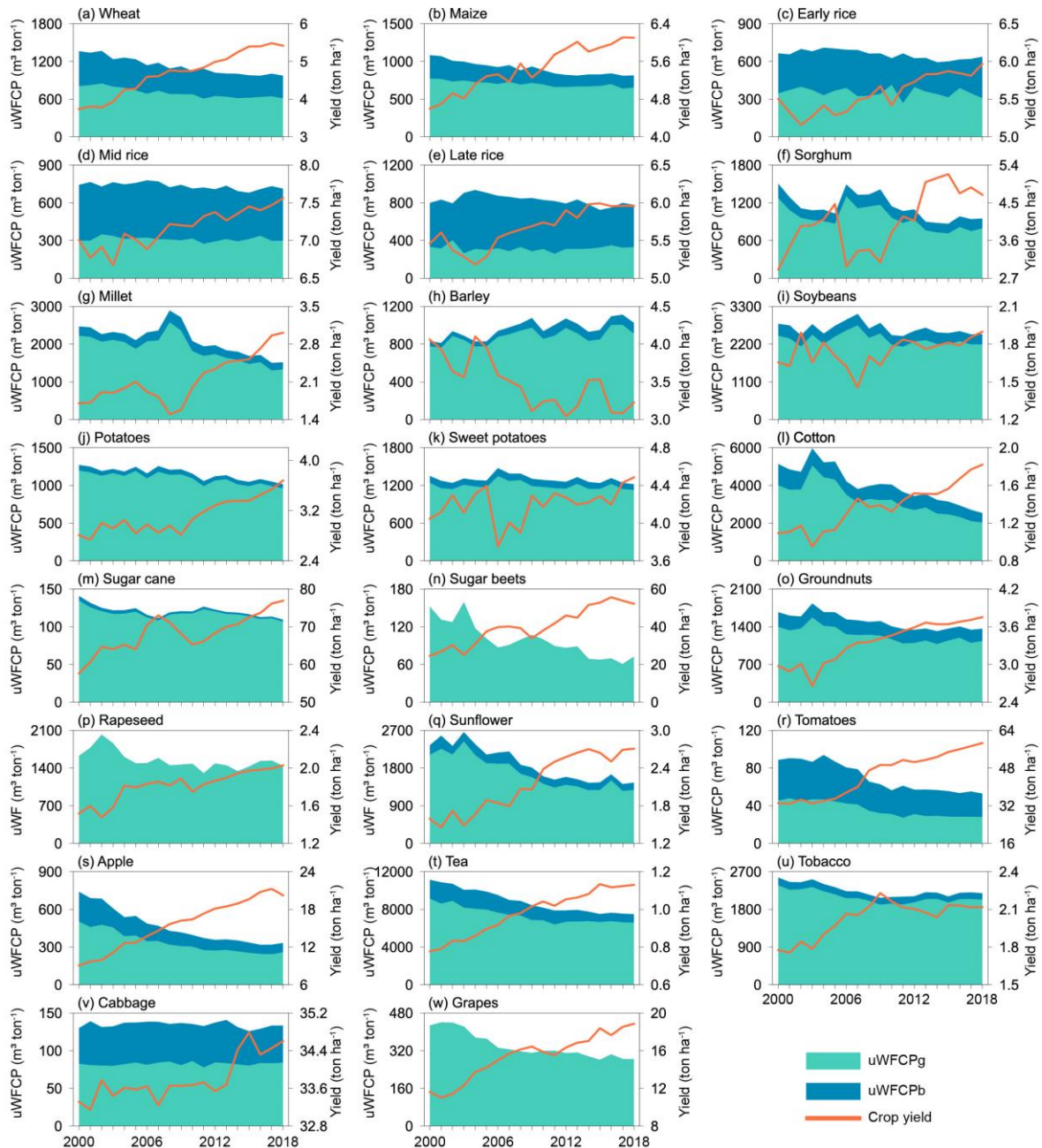
310

period as yield grew (Fig. 4). The uWFCP of cotton (51%), sugar beets (52%), and apple (55%) showed the greatest reduction.

311

The uWFCP of wheat and maize decreased by more than 25%, because the yield increased by 45% and 33%, respectively.

312



313

314

Figure 4. Interannual variation in uWFCPb, uWFCPg, and yield of 21 crops in China over 2000-2018.

315 The uWFCP of the 21 crops was relatively high under rain-fed conditions (Table 4, Fig. S15). Additionally, the uWFCP<sub>b</sub>,  
316 uWFCP<sub>g</sub>, and yield of each crop responded differently to the three irrigation treatments. These variations were caused by the  
317 fact that the proportions of blue and green water consumption via soil evaporation and crop transpiration differed between  
318 crops and irrigation practices (Fig. S16). For example, blue water consumption via crop transpiration in furrow and sprinkler  
319 irrigation accounted for 45% and 51% of the total crop water consumption, respectively, which was much lower than that of  
320 micro-irrigation (62%). Therefore, the effects of different water supply modes and irrigation practices should be considered in  
321 the quantification of uWFCP over a long time series.

322

323 **Table 4. The uWFCP<sub>b</sub>, uWFCP<sub>g</sub>, and yield of 21 crops under different water supply modes and irrigation practices in 2018.**

Crop	Furrow irrigation			Micro irrigation			Sprinkler irrigation			Rain-fed	
	Blue uWFCP m <sup>3</sup> ton <sup>-1</sup> (△)	Green uWFCP m <sup>3</sup> ton <sup>-1</sup> (△)	Yield ton ha <sup>-1</sup> (△)	Blue uWFCP m <sup>3</sup> ton <sup>-1</sup> (△)	Green uWFCP m <sup>3</sup> ton <sup>-1</sup> (△)	Yield ton ha <sup>-1</sup> (△)	Blue uWFCP m <sup>3</sup> ton <sup>-1</sup> (△)	Green uWFCP m <sup>3</sup> ton <sup>-1</sup> (△)	Yield ton ha <sup>-1</sup> (△)	Green uWFCP m <sup>3</sup> ton <sup>-1</sup> (△)	Yield ton ha <sup>-1</sup> (△)
Wheat	508 (-30%)	447 (-18%)	6.1 (36%)	628 (-18%)	340 (-29%)	5.1 (20%)	636 (-31%)	464 (-16%)	5.5 (35%)	999 (-38%)	4.5 (80%)
Maize	369 (-26%)	477 (-15%)	6.4 (25%)	369 (-26%)	238 (-52%)	9.4 (80%)	390 (-38%)	396 (-24%)	7.3 (39%)	820 (-26%)	5.7 (43%)
Early rice	231 (4%)	406 (-6%)	0.2 (463%)	–	–	–	332 (4%)	305 (-12%)	172.6 (-79%)	–	–
Mid rice	349 (-24%)	382 (-4%)	0.6 (361%)	–	–	–	420 (-5%)	291 (-2%)	91.7 (-73%)	–	–
Late rice	237 (8%)	540 (-2%)	0.2 (526%)	–	–	–	454 (-3%)	322 (-2%)	156.6 (-81%)	–	–
Sorghum	601 (-43%)	793 (-29%)	3.7 (54%)	713 (-21%)	567 (-42%)	3.8 (52%)	693 (-56%)	696 (-39%)	3.9 (82%)	805 (-39%)	5.2 (67%)
Millet	719 (-45%)	807 (-32%)	3.5 (65%)	705 (-36%)	531 (-47%)	3.8 (68%)	712 (-51%)	652 (-38%)	4.0 (76%)	1,528 (-38%)	2.8 (75%)
Barley	369 (15%)	536 (15%)	3.7 (-7%)	660 (86%)	558 (55%)	2.9 (-26%)	1,038 (117%)	1,069 (130%)	2.1 (-48%)	1,051 (25%)	3.1 (-24%)
Soybeans	915 (-14%)	1,569 (-8%)	2.2 (12%)	1,359 (-1%)	1,236 (-19%)	2.1 (14%)	1,006 (-29%)	1,575 (6%)	2.0 (2%)	2,489 (-11%)	1.8 (16%)
Potatoes	192 (-10%)	258 (25%)	9.9 (-22%)	188 (-14%)	105 (-30%)	19.0 (31%)	156 (-3%)	150 (42%)	17.0 (-24%)	1,253 (-28%)	2.9 (47%)
Sweet potatoes	403 (-26%)	762 (-7%)	5.1 (14%)	485 (-22%)	751 (-3%)	4.9 (11%)	457 (-38%)	721 (4%)	5.2 (9%)	1,231 (-8%)	4.3 (10%)
Cotton	2,539 (-18%)	2,623 (-3%)	1.4 (17%)	1,306 (-53%)	360 (-80%)	4.5 (208%)	2,807 (-22%)	2,704 (20%)	1.3 (3%)	2,133 (-55%)	1.8 (71%)
Sugar cane	16 (-31%)	37 (-32%)	164.9 (56%)	13 (-10%)	29 (-17%)	200.7 (26%)	19 (-43%)	41 (-41%)	146.1 (83%)	120 (-26%)	69.8 (40%)
Sugar beets	8 (-35%)	2 (-36%)	752.3 (54%)	7 (-35%)	2 (-32%)	786.0 (49%)	10 (-26%)	4 (-23%)	520.9 (30%)	72 (-53%)	52.2 (114%)
Groundnuts	440 (-35%)	608 (-29%)	5.5 (50%)	633 (0%)	540 (-10%)	5.0 (11%)	534 (-41%)	567 (-14%)	5.5 (32%)	1,669 (-5%)	2.8 (8%)
Rapeseed	181 (35%)	611 (-48%)	6.0 (58%)	116 (19%)	676 (-39%)	6.0 (52%)	181 (35%)	611 (-48%)	6.0 (58%)	1,435 (-12%)	2.0 (34%)

Sunflower	829	639	3.6	694	250	6.0	794	485	4.5	1,504	2.4
	(-27%)	(-6%)	(21%)	(-42%)	(-62%)	(121%)	(-30%)	(-13%)	(28%)	(-39%)	(72%)
Tomatoes	25	28	58.6	28	22	58.7	27	25	58.6	–	–
	(-43%)	(-38%)	(77%)	(-41%)	(-39%)	(77%)	(-52%)	(-31%)	(77%)	–	–
Apple	159	150	26.1	200	128	20.9	219	177	21.1	345	17.5
	(-65%)	(-56%)	(159%)	(-40%)	(-54%)	(87%)	(-66%)	(-55%)	(151%)	(-48%)	(111%)
Tea	1,769	2,552	2.3	1,546	2,601	2.2	1,620	2,218	2.6	10,769	0.7
	(-52%)	(-57%)	(138%)	(-64%)	(-66%)	(221%)	(-65%)	(-63%)	(198%)	(-17%)	(17%)
Tobacco	596	1,303	2.6	486	1,436	2.2	622	1,110	2.9	2,281	2.0
	(-25%)	(-5%)	(13%)	(-24%)	(13%)	(-14%)	(-40%)	(9%)	(6%)	(-15%)	(20%)
Cabbage	49	85	34.7	53	71	32.7	48	79	35.0	–	–
	(4%)	(2%)	(4%)	(6%)	(-7%)	(-2%)	(-14%)	(9%)	(5%)	–	–
Grapes	135	63	33.8	115	54	33.8	148	64	33.8	283	18.8
	(-44%)	(-45%)	(80%)	(-45%)	(-46%)	(80%)	(-44%)	(-45%)	(80%)	(-34%)	(63%)

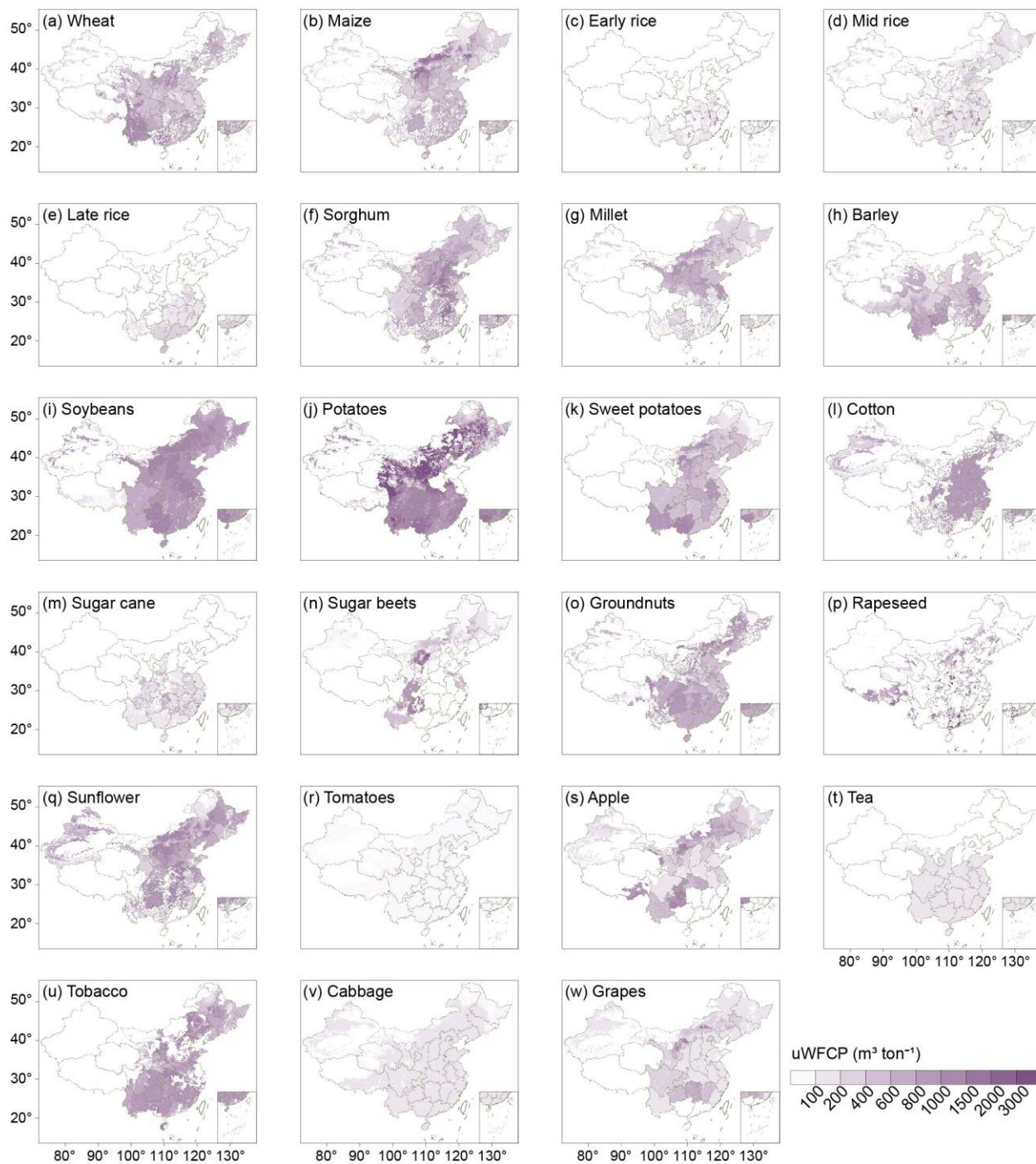
324 Note: “ $\Delta$ ” refers to the rate of change from 2000 to 2018. “-” indicates that no crops are grown.

325

326 The spatial distribution of the gridded uWFCP showed significantly heterogeneity (Fig. 5, S17, and S18). There were  
327 many regions with high-gridded uWFCP values for potatoes, which were concentrated in northern China. The crop with the  
328 densest distribution of high-gridded uWFCP<sub>b</sub> values was tea, which was commonly dispersed throughout the southern regions.  
329 Soybean and millet possessed more uWFCP<sub>g</sub> high-value areas, mainly in the northern regions. By comparing the relative  
330 changes in the average grid uWFCP from the period of 2000-2009 to that of 2010-2018, it was determined that the uWFCP of  
331 all 21 crops exhibited a spatially significant decreasing trend (Fig. S19–S21). It is essential to emphasise that the dominant  
332 factors governing this decrease in uWFCP varied among crops. For example, the decline observed in the uWFCP of apple was  
333 attributable to a substantially larger decrease in uWFCP<sub>g</sub> than the corresponding rise in uWFCP<sub>b</sub>, whereas that observed for  
334 tea was caused by a considerable decrease in uWFCP<sub>b</sub>.

335 For most crops, rainfed ones had more regions of high uWFCP than irrigated ones, and the geographical distribution of  
336 uWFCP for the same crop was generally consistent, regardless of irrigation practices. The variation in uWFCP<sub>b</sub> and uWFCP<sub>g</sub>  
337 for the same water supply mode and irrigation practice in a crop was considerable owing to regional water consumption and  
338 yield differences (Fig. S22 and S23). Additionally, the temporal evolution of uWFCP<sub>b</sub> and uWFCP<sub>g</sub> under various water supply  
339 modes and irrigation practices was analysed, and rainfed crops demonstrated a more rapid and wider reduction in uWFCP than  
340 irrigated crops.

341



342

343 **Figure 5. Gridded uWFCP of 21 crops in China at annual average level for 2000-2018.**

344

345 **3.3 Benchmarks for uWFCP**

346

347

348

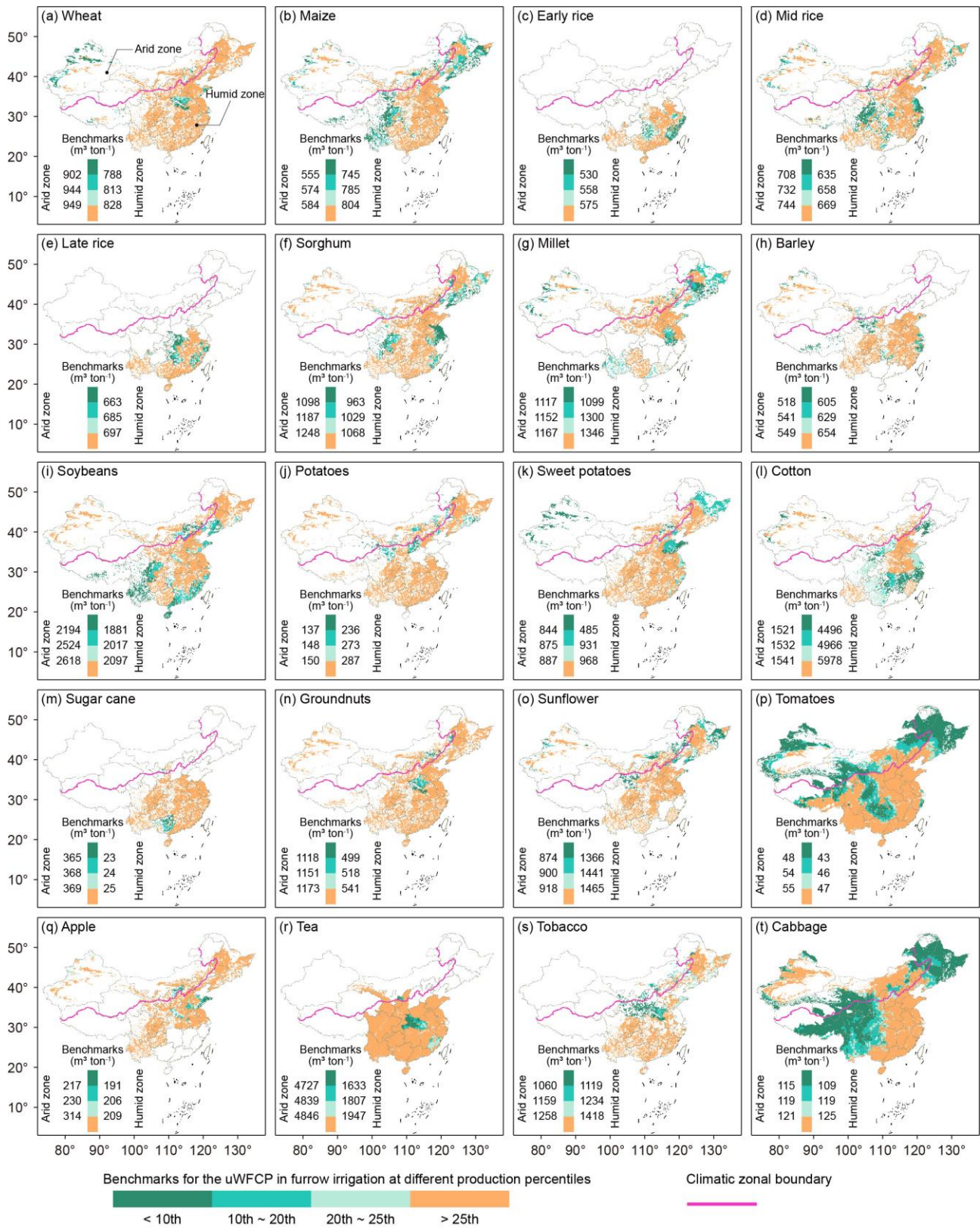
349

Annual uWFCP benchmarks were calculated using the different production percentiles for each of the 21 crops under various water supply modes and irrigation practices. Significant interannual differences existed between these uWFCP benchmarks, therefore, we reassessed these benchmarks using whole time series measurements to reduce the impact of anomalous values resulting from extreme climate events. The crops uWFCP benchmarks in Table S1 can be selected as a

350 reference for future analysis like Yue et al. (2022). Results show that benchmarks for the uWFCP of different crops responded  
351 differently to climatic zone. Crops such as millet, soybeans, and groundnuts had higher benchmarks for uWFCP in arid zones  
352 than in humid zones due to differences in production percentiles; the reverse was true for maize, cotton, and sunflower. Several  
353 factors contribute to these results. Firstly, crops cultivated in arid zones are more irrigation-reliant due to scarce precipitation  
354 and undergo greater evapotranspiration, resulting in higher uWFCP versus humid zones. Secondly, certain crops like cotton  
355 possess higher benchmarks in humid zones since their yields are markedly lower than those extensively grown in arid regions.  
356 Overall, the uWFCP benchmarks for rainfed crops were higher than those for irrigated crops. The uWFCP benchmarks for  
357 each irrigation practice varied by crop species.

358 Fig. 6 and Fig. S26–S28 present the uWFCP benchmarks according to different production percentiles in humid and arid  
359 zones and as obtained for various water supply modes and irrigation practices. Except for vegetables (tomatoes and cabbage),  
360 the majority of crops were cultivated in regions with a uWFCP benchmark that exceeded the 25% production percentile. Under  
361 furrow and sprinkler irrigation, the areas that fell below the uWFCP benchmark at the 25% production percentile were  
362 predominantly distributed in the humid zone. In the arid zone, a greater proportion of micro-irrigated regions fell below the  
363 uWFCP benchmark at the 25% production percentile. The results indicate that governing bodies need to consider the influence  
364 of climatic zones as well as water supply modes and irrigation practices when quantifying uWFCP benchmarks to identify  
365 hotspots for water-saving potential; specific water-use policies need to be formulated both for crop varieties and irrigation  
366 practices.

367



368

369

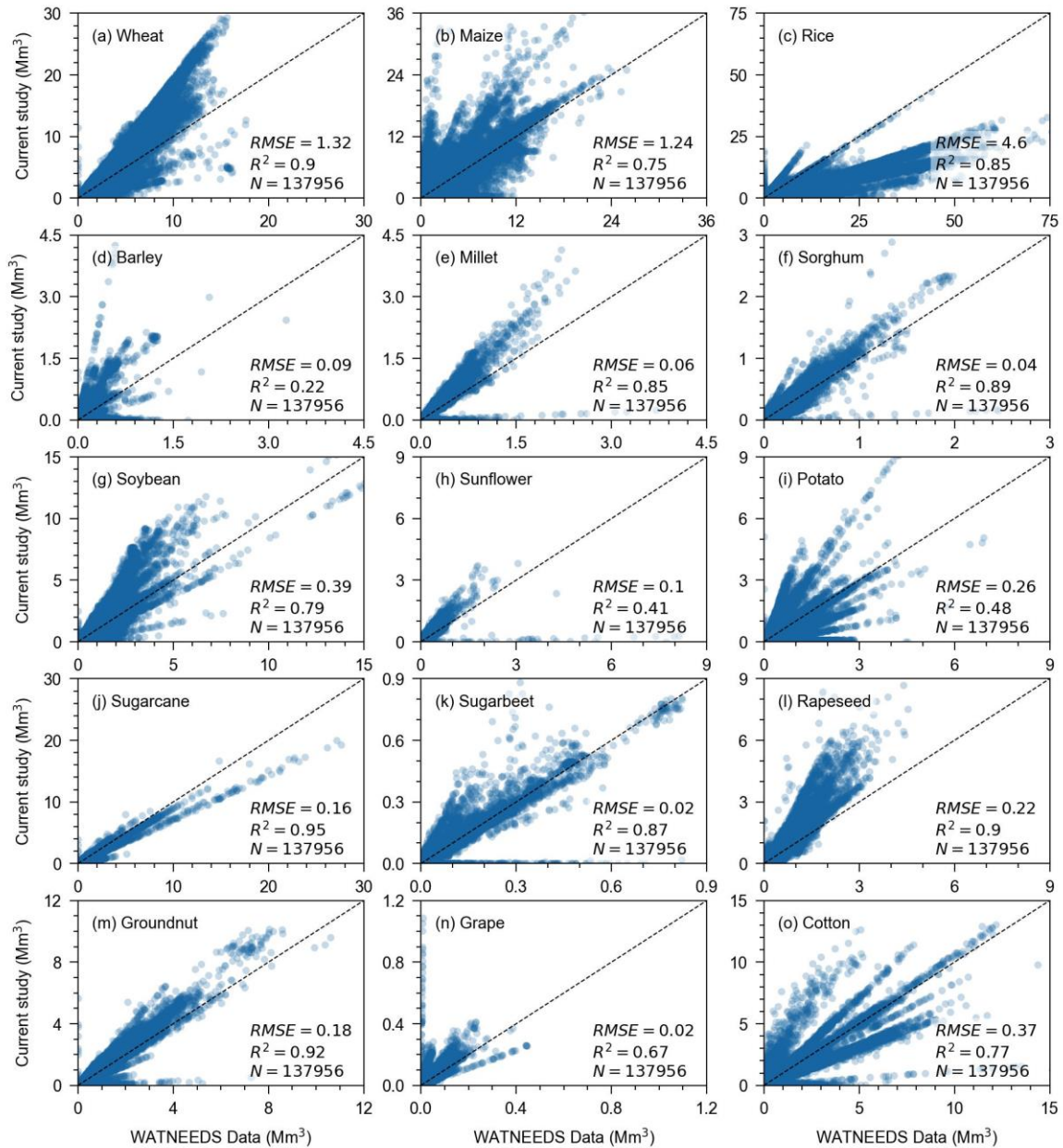
Figure 6. Benchmarks for uWFCP at different production percentiles under furrow irrigation in China by 2018.

370

### 371 3.4 Results comparison

372 Using publicly available datasets, we compared the water use of 15 crops with the WATNEEDS dataset (Chiarelli et al.,  
373 2020) that overlapped in time (in 2000) and space (137,956 grids). As illustrated in Fig. 7, the results showed that  $R^2 > 0.60$  ( $p$   
374  $< 0.01$ ) among 12 of the crops. However, large deviations were present in the comparisons of data for barley, sunflower, and  
375 potatoes. The following two factors were responsible for this disparity. First, the current study aimed to quantify the actual  
376 water consumption during crop growth, whereas the WATNEEDS dataset concentrated on theoretical crop water requirements.  
377 Second, this study divided irrigation into furrow, sprinkler, and micro-irrigation categories at the grid scale. In reality, sprinkler  
378 irrigation covers a much larger area than micro-irrigation does and also possesses the highest  $f_w$  of our three irrigation categories,  
379 which is ultimately reflected in a higher water consumption in our data. Overall, our dataset displayed a high level of reliability.  
380 The comparison of our WFCP data with the WATNEEDS dataset (Chiarelli et al., 2020) on a national scale is shown in Table  
381 5. Except for rice, the variability of WFCP and WFCP<sub>b</sub> between the two datasets was under 25% and 20%, respectively,  
382 demonstrating high consistency. Large differences in the WFCP<sub>g</sub> between the two datasets can be attributed to two factors,  
383 namely, the different quantification methods used (including model mechanisms and green water definitions) and the different  
384 sources of precipitation data used for model input, leading to variations in green water simulations. With regards to the  
385 variability observed in rice data, some of our grids contained information for two to three seasons of rice cultivation (combined  
386 with the actual regional cultivation), and all these instances were assumed to receive irrigation in this study; this may have  
387 resulted in a comparatively low WFCP<sub>g</sub> value.

388



389  
 390 **Figure 7. Comparison of WFCP with WATNEEDS dataset.**

391  
 392 In a comparison of the uWFCP obtained for 21 crops in our dataset with figures reported by Mekonnen and Hoekstra  
 393 (2011) and Zhuo et al. (2016a), the variability of data for 18 crops was under 30%, which was attributed to the uncertainty  
 394 imposed by model simulation (Table 5). Although crop acreage remains consistent at the national scale, sets of crop distribution  
 395 data must be matched with different sets of input variables (such as precipitation, temperature, and soil moisture content),  
 396 which has a significant impact on the simulated values. The differences in the uWFCP of potato, sweet potato, and cotton  
 397 resulted from the large discrepancies in production data, with simulated values for these three crops by Mekonnen and Hoekstra  
 398 (2011) and Zhuo et al. (2016a) being 80%, 81%, and 67% higher than the statistical yearbook.



400 **Table 5. Comparison of WFCP and uWFCP in overlapping time and space with published results.**

Crop	WFCP					uWFCP					uWFCP				
	Unit: M m <sup>3</sup> yr <sup>-1</sup> . Period: 2000.					Unit: m <sup>3</sup> ton <sup>-1</sup> . Period: 2000-2005.					Unit: m <sup>3</sup> ton <sup>-1</sup> . Period: 2000-2009.				
	Current study		Chiarelli et al., 2020		( $\Delta$ )	Current study		Mekonnen and Hoekstra, 2011		( $\Delta$ )	Current study		Zhuo et al., 2016a		( $\Delta$ )
Blue	Green	Blue	Green		Blue	Green	Blue	Green		Blue	Green	Blue	Green		
Wheat	80	55	79	22	(14%)	800	501	821	466	(1%)	754	472	1,135	392	(11%)
Maize	82	33	78	24	(6%)	744	264	791	74	(8%)	728	239	747	56	(9%)
Rice	59	80	255	97	(43%)	328	432	549	246	(2%)	323	437	987	395	(29%)
Sorghum	3	1	3	0	(4%)	1,002	178	952	42	(9%)	1,059	186	695	58	(25%)
Millet	5	1	4	0	(11%)	2,092	224	1,600	40	(17%)	2,145	242	1,418	141	(21%)
Barley	3	0	4	0	(21%)	804	50	556	28	(19%)	843	58	560	120	(14%)
Soybeans	38	5	33	5	(5%)	2,337	326	2,549	249	(2%)	2,418	317	2,336	316	(2%)
Potatoes	16	1	16	1	(0%)	1,163	62	215	7	(69%)	1,154	64	183	9	(73%)
Sweet potatoes	29	3				1,184	105	242	4	(68%)	1,211	108	63	22	(88%)
Cotton	18	5	23	3	(8%)	4,236	951	1,440	247	(51%)	3,781	847	1,117	281	(54%)
Sugar cane	9	0	12	1	(17%)	122	5	169	6	(16%)	118	4	124	1	(1%)
Sugar beets	1	0	1	0	(2%)	130	0	148	0	(6%)	117	0	104	0	(6%)
Groundnuts	20	4	19	3	(5%)	1,412	257	1,383	85	(6%)	1,347	260	1,399	219	(0%)
Rapeseed	18	0	12	0	(22%)	1,713	0	1,387	0	(11%)	1,623	0	1,754	0	(4%)
Sunflower	4	0	3	0	(9%)	2,154	232	2,254	341	(4%)	1,991	237	1,025	163	(30%)
Tomatoes	1	1				46	43	182	3	(35%)	42	39	81	2	(2%)
Apple	10	5				443	186	796	30	(14%)	389	154	372	46	(13%)
Tea	6	1				8,440	1,970	9,277	798	(2%)	7,860	1,792	9,055	122	(3%)
Tobacco	6	0				2,273	174	2,007	253	(4%)	2,162	167	1,771	18	(13%)
Cabbage	3	2				82	53	237	4	(28%)	82	53	122	8	(2%)
Grapes	1	0	1	0	(7%)	407	0	357	0	(7%)	364	0	349	123	(13%)

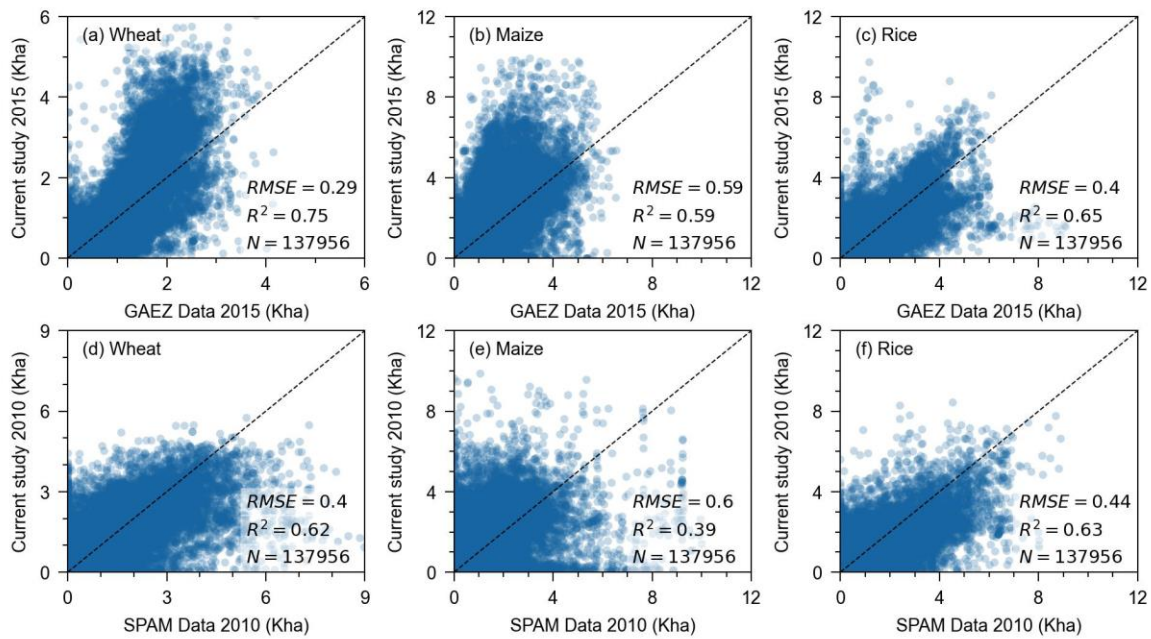
401 Note: “ $\Delta$ ” Calculated as the ratio of the study difference to the study mean.

402

403 **4 Discussion**404 **4.1 Data validation**

405 We compared our 5 arcmin resolution of major crop areas, as calculated by the proportional invariant method, with the  
406 GAEZ+ (Grogan et al., 2022) and SPAM (IFPRI, 2019) data products in the same year (Fig. 8). Linear regression results for  
407 data on wheat, maize, and rice coverage showed that  $R^2$  was greater than 0.50 ( $p < 0.01$ ) at the raster scale and greater than  
408 0.80 ( $p < 0.01$ ) at the provincial scale, and the overall variability at the national scale was under 8%. We further compared

409 planting areas of other crops in SPAM and our data provincially and in grids (Fig. S29 and S30). It is evident that there is a  
 410 high  $R^2$  at the provincial scale. The differences at the grid scale can be attributed to discrepancies in the identification of gridded  
 411 land use between the MIRCA2000 and SPAM. According to Fig. S31 and S32, the planting area data for sorghum, millet,  
 412 barley, and sugar beets in the GAEZ+ exhibit significant deviations from this study, both at the provincial and grid scales.  
 413 However, it should be emphasized that all crop planting area data in this study have been calibrated against statistical data at  
 414 the provincial scale, implying an underestimation of the planting area for the mentioned crops in the GAEZ+. Overall,  
 415 comparisons with existing products validated the accuracy of the gridded representation of crop land coverage as obtained in  
 416 this study.  
 417

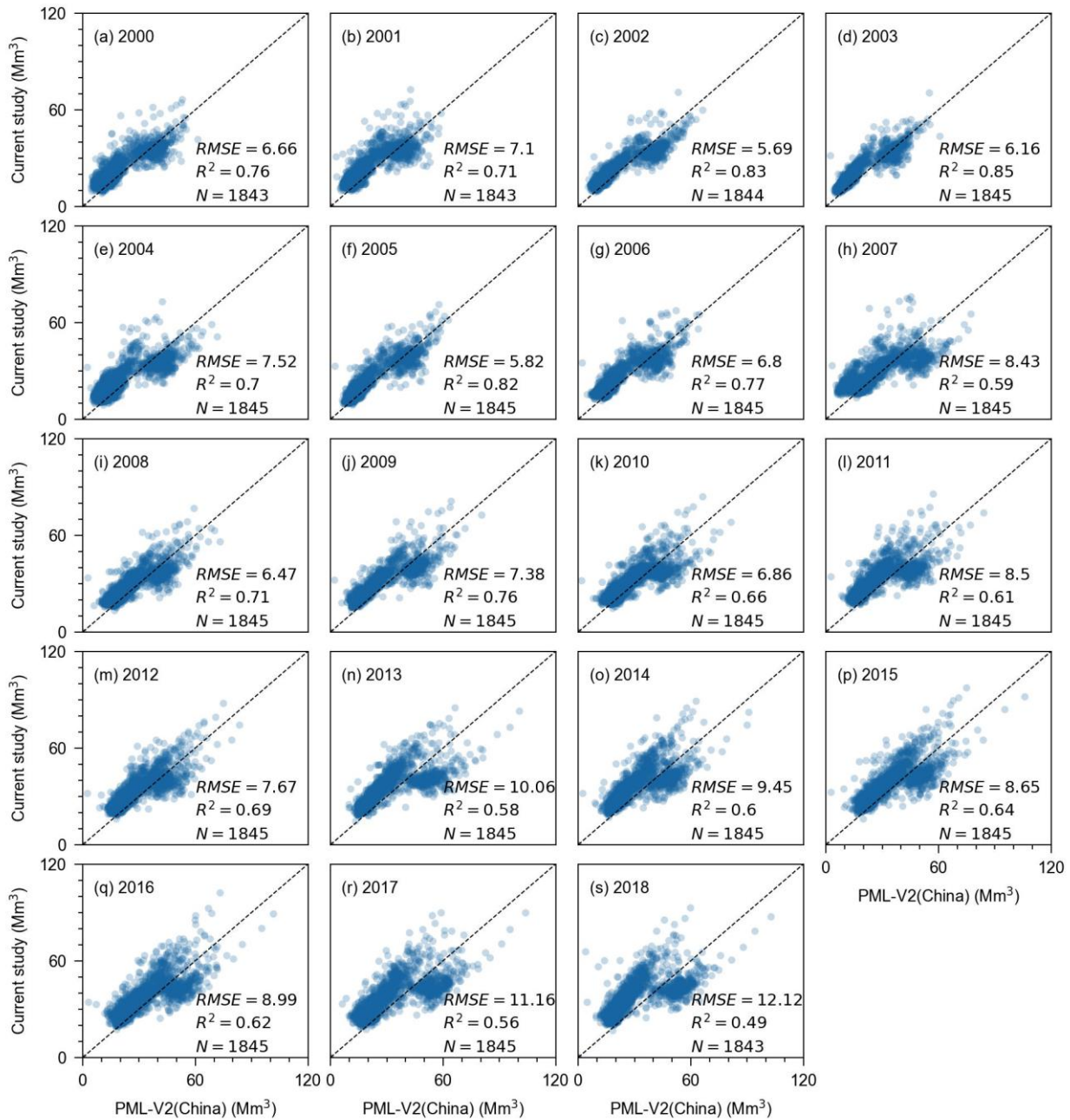


418  
 419 **Figure 8. Comparison of the current gridded area representing land coverage by major crops with the GAEZ+ and SPAM datasets.**

420  
 421 Based on data from dual-source (PML-V2(China)) and single-source (SEBAL) remote sensing products, we validated  
 422 our evapotranspiration, evaporation and transpiration results specifically over the major cropping period from April to August  
 423 by following the selection process outlined in Section 2.3.2. Comparative analysis in Fig.9 and Fig. S33 revealed stronger  
 424 agreement between the simulated evapotranspiration and the PML-V2 products ( $R^2=0.49 - 0.85$ ,  $RMSE=5.82 - 12.12$   $Mm^3$ )  
 425 than those with the SEBAL products ( $R^2= 0.44 - 0.75$ ,  $RMSE=8.51 - 15.82$   $Mm^3$ ), although both comparisons demonstrated  
 426 robust overall consistency. The validation results of soil evaporation ( $E$ ) are presented in Fig. S34. The simulated  $E$  were  
 427 marginally lower than the PML-V2 products ( $R^2=0.22 - 0.70$ ,  $RMSE=3.25 - 6.65$   $Mm^3$ ), owing to the current study calculating  
 428  $E$  exclusively for the planted regions of 21 crops, whereas the PML-V2 disregarded land use types during  $E$  estimation.

429 Comparative analysis of crop transpiration in Fig. S35 indicated that our simulated values were higher than the PML-V2  
 430 products which deducted canopy evaporation ( $R^2=0.38 - 0.69$ ,  $RMSE=6.04 - 10.35$   $Mm^3$ ). Overall, considering the differences  
 431 in basic input data, spatiotemporal resolution and calculation methods, the evapotranspiration, evaporation, and transpiration  
 432 data products produced in this study showed acceptable results when compared with various remote sensing products, given  
 433 the discrepancies exhibited.

434



435

436 **Figure 9. Validation of the evapotranspiration at croplands for the period April to August with PML-V2(China) datasets.**

437

439 To clarify the sensitivity of a WFCP assessment to the main parameters in a simulation, a previous study by the authors  
440 applied the one-at-a-time and sensitivity index methods to quantitatively evaluate a WFCP calculation by AquaCrop (Li et al.,  
441 2022). The results indicated that crop water consumption and production were extremely sensitive to the reference  
442 evapotranspiration, planting date (PD) and the crop transpiration coefficient (KcTr). The effect of PD differed for each crop,  
443 and advancing or delaying it exposed crops to completely different rain and heat conditions. Minor shifts in PD forward or  
444 backward have relatively small influences on WFCP since crop water consumption is primarily concentrated in crop  
445 development and mid-season stages (Table S4 and Fig. S36). Moreover, yield and WFCP exhibited minimal sensitivity to  
446 changes in crop PD when preserving constant growing degree days (Zhuo et al., 2014). In the Annex of the Reference manual  
447 for the AquaCrop (Raes et al., 2018), default values of crop parameters for the crops covered in this study are given, including  
448 crop transpiration, biomass production and yield formation, and stresses, totalling 41 parameters. Furthermore, these  
449 parameters are further classified based on crop sensitivity as conservative generally applicable (including KcTr), conservative  
450 for a given species but can or may be cultivar specific, dependent on environment and/or management and cultivar specific.  
451 The conservative parameters are generally applicable and remain unchanged across a wide spectrum of conditions, including  
452 different climatic and geographic locations, crop cultivars and genotypes, as well as variable soil moisture stress statuses. Once  
453 calibrated, these identical parameters would be utilized without further modification. Importantly, the accuracy of all model  
454 studies (including those using AquaCrop) is dependent on both the model mechanism and the input data. AquaCrop's accuracy  
455 in simulating crop water consumption and production for various climates, soils, and field management practices has been  
456 extensively validated (Zhuo et al., 2016a; Pirmoradian and Davatgar, 2019; Wang et al., 2019; Chibarabada et al., 2020).

457 At the outset of the simulation used in this study, we rigorously screened the input data according to the principles of  
458 accuracy and representativeness. However, there was a degree of bias in the model setup and input data. For instance, the  
459 current study focused on the effect of water stress on crop growth and worked from the assumption that all nutrients required  
460 for crops were provided. Firstly, AquaCrop, as a water-driven model, simulates crop growth comprehensively by establishing  
461 the responsive link between effective soil water usage and crop yield (Raes et al., 2018). Secondly, AquaCrop adopts a semi-  
462 quantitative method to evaluate fertilizer stress. That is, it cannot directly simulate crop response to fertilizer based on plant  
463 nutritional demand and soil nutrient content (Akumaga et al., 2017). Research shows AquaCrop performs better without  
464 fertilizer stress versus with stress (Adeboye et al., 2021; Wu et al., 2022). In fact, there is a serious overapplication of chemical  
465 fertilisers in Chinese farmlands (Chen et al., 2014; Cui and Shoemaker, 2018). The impact of fertilization on crop production  
466 was indirectly reflected through calibration against statistical data. Thirdly, gridded data is deficient regarding fertilizer

467 varieties and application quantities, more so for crop-specific data. So like past AquaCrop global (Mialyk et al., 2022) and  
468 national (Wang et al., 2019) studies, nutrient stress is not considered in simulations. Certainly, the above assumption has  
469 limitations. Establishing high resolution fertilizer application databases is vital for future crop production research.

470 Furthermore, the parameters we used for fraction of the surface wetted in either furrow, sprinkler, or micro-irrigation  
471 remained consistent across regions owing to the absence of any data related to possible variance as mentioned in section 2.2.5;  
472 in other words, we downplayed regional variations within the same irrigation practice. Taking micro-irrigation as an example,  
473 the difference between different micro-irrigation products mostly lies in the transport and distribution pipe networks and  
474 irrigator, which have little impact on the fraction of the surface wetted in the crop root zone. In terms of crop parameters, strict  
475 regional differences were considered during the initial screening of the 21 crops' parameters. According to the regional  
476 classification results in Table S3, these key parameters like plant dating, reference harvest index, crop growth stages, and  
477 maximum root depth for this study are obtained by referring to the literatures described in section 2.1.3. These data have been  
478 validated to be reliable and applicable in large-scale studies (Cao et al., 2014; Zhuo et al., 2016a; Wang et al., 2019). Due to  
479 data limitations, the remaining parameters such as maximum canopy cover, canopy cover decline coefficient, canopy growth  
480 coefficient were assigned the mean values within the reference range provided in the Annex of the Reference manual for the  
481 AquaCrop. Although this approach may overlook certain potential variations, the use of mean values generally captures the  
482 central tendency of the data.

483 Unlike small-scale studies at site level that emphasize region-specific measured parameters for model simulation, large  
484 regional-scale studies often adopt literature-recommended parameter values during data collection, with greater focus on  
485 regional variability and wide adaptability of the parameters. (Hoekstra and Wiedmann 2014; Davis et al., 2017; Mekonnen and  
486 Hoekstra 2020; Lutz et al., 2022; Halpern et al., 2022; Liu et al., 2022; Chiarelli et al., 2022; Demay et al., 2023). It was neither  
487 practical nor feasible to calibrate crop parameters individually for each grid given the constraints of available data.  
488 Nevertheless, we have made every effort to ensure the reliability of the model input parameters within the existing limitations.  
489 Consequently, in future research, attention to the collection and organisation of basic data can play a positive role in the  
490 improvement of the model mechanism and accuracy of the output (Mekonnen and Hoekstra, 2010; Mekonnen and Hoekstra,  
491 2011).

492 In general, despite the uncertainties in the input data, the calculated WFCP and uWFCP were in good agreement with  
493 existing studies at both the grid and national scales, and the dataset in the long time series was compatible with remote sensing  
494 products. The above analysis demonstrated that the findings of our current study correctly reflected water consumption during  
495 the crop growth period under various water supply modes and irrigation practices.

## 496 **5 Data availability**

497 All data used in this study are freely available with the links given in Sect. 2. The dataset presented in this article are  
498 available from the Zenodo repository at <https://doi.org/10.5281/zenodo.7756013> (Wang et al., 2023). Both gridded  
499 consumptive water footprints, evaporation, transpiration, and associate benchmarks of crop production are provided.

## 500 **6 Conclusions**

501 The current study constructed a gridded WFCP database for 21 crops in China for 2000-2018 to reflect different water  
502 supply modes and irrigation practices, thereby addressing monthly blue and green water consumption in soil evaporation and  
503 crop transpiration. Additionally, we established uWFCP benchmarks for various climatic zones, water supply modes and  
504 irrigation practices. The current dataset was thoroughly validated. The results highlighted the necessity to explore the  
505 influences of different field management practices on WFCP quantification and benchmarking in future research.

506 The WFCP is a crucial indicator used for evaluating water consumption by crops and a key component to solving the  
507 problems associated with the environmental "footprint family" and "planetary boundary" (Galli et al., 2012; Hoekstra and  
508 Wiedmann, 2014; Steffen et al., 2015). The current dataset is able to support for precise crop water productivity assessments,  
509 agricultural water-saving evaluations, the development of sustainable irrigation techniques, cropping structure optimisation,  
510 and crop-related interregional virtual water trade analysis. The dataset can furthermore be applied to develop dynamic water  
511 management policies by virtue of its analysis of the spatial and temporal fluctuations in crop water consumption. The  
512 methodological framework for batch quantification of the WFCP can facilitate the updating of relative dataset and scale  
513 conversion studies.

## 514 **Author contributions**

515 LZ and PW designed the research. WW collected basic data, performed simulations, and conducted results validation and  
516 calibration. XJ conducted the sensitivity analysis. ZY, ZL, ML, HZ, RG, CY, and PZ performed simulations. WW and LZ  
517 wrote the original manuscript. LZ and PW revised the manuscript.

## 518 **Competing interests**

519 The contact author has declared that neither they nor their co-authors have any competing interests.

520 **Acknowledgements**

521 We thank all colleagues for their support and work. The dataset could not be established without the contributions of all  
522 participants.

523 **Financial support**

524 The study is financially supported by the Program for Cultivating Outstanding Talents on Agriculture, Ministry of  
525 Agriculture and Rural Affairs, People's Republic of China (13210321), the National Youth Talents Plan, and Chinese  
526 Universities Scientific Fund (2452021168) to LZ.

527 **References**

- 528 Adeboye, O. B., Schultz, B., Adeboye, A. P., Adekalu, K. O., and Osunbitan, J. A.: Application of the AquaCrop model in  
529 decision support for optimization of nitrogen fertilizer and water productivity of soybeans, *Inf. Process*, 8(3), 419-436,  
530 <https://doi.org/10.1016/j.inpa.2020.10.002>, 2021.
- 531 Akumaga, U., Tarhule, A., and Yusuf, A. A.: Validation and testing of the FAO AquaCrop model under different levels of  
532 nitrogen fertilizer on rainfed maize in Nigeria, West Africa, *Agr. Forest Meteorol.*, 232, 225-234,  
533 <https://doi.org/10.1016/j.agrformet.2016.08.011>, 2017.
- 534 Allen, R. G., Pereira, L. S., Raes, D., and Smith, M.: Crop evapotranspiration—Guidelines for computing crop water  
535 requirements-FAO Irrigation and drainage paper 56, 300, D05109, FAO, Rome, 1998.
- 536 Batjes, N. H.: ISRIC-WISE derived soil properties on a 5 by 5 arc-minutes global grid (ver. 1.2), ISRIC-World Soil Information,  
537 available at: <https://data.isric.org/geonetwork/srv/eng/catalog.search#/metadata/82f3d6b0-a045-4fe2-b960-6d05bc1f37c0>. (last access: 7 March 2023), 2012.
- 539 Brown, J. F. and Pervez, M. S.: Merging remote sensing data and national agricultural statistics to model change in irrigated  
540 agriculture, *Agric. Syst.*, 127, 28-40, <https://doi.org/10.1016/j.agry.2014.01.004>, 2014.
- 541 Cao, X., Wu, P., Wang, Y., and Zhao, X.: Assessing blue and green water utilisation in wheat production of China from the  
542 perspectives of water footprint and total water use, *Hydrol. Earth Syst. Sci.*, 18(8), 3165-3178,  
543 <https://doi.org/10.5194/hess-18-3165-2014>, 2014.
- 544 Chen, X., Cui, Z., Fan, M., Vitousek, P., Zhao, M., Ma, W., Wang, Z., Zhang, W., Yan, X., and Yang, J.: Producing more grain  
545 with lower environmental costs, *Nature*, 514, 486-489, <https://doi.org/10.1038/nature13609>, 2014.

- 546 Chen, Y., Guo, G., Wang, G., Kang, S., Luo, H., and Zhang, D.: Main crop water requirement and irrigation of China, Hydraulic  
547 and Electric Press, Beijing, 1995.
- 548 Cheng, M., Jiao, X., Li, B., Yu, X., Shao, M., and Jin, X.: Long time series of daily evapotranspiration in China based on the  
549 SEBAL model and multisource images and validation, *Earth Syst. Sci. Data*, 13, 3995-4017, [https://doi.org/10.5194/essd-](https://doi.org/10.5194/essd-13-3995-2021)  
550 13-3995-2021, 2021.
- 551 Chiarelli, D. D., Passera, C., Rosa, L., Davis, K. F., D'Odorico, P., and Rulli, M. C.: The green and blue crop water requirement  
552 WATNEEDS model and its global gridded outputs, *Sci. Data*, 7, 273, <https://doi.org/10.1038/s41597-020-00612-0>, 2020.
- 553 Chiarelli, D. D., D'Odorico, P., Müller, M. F., Mueller, N. D., Davis, K. F., Dell'Angelo, J., Penny, G., and Rulli, M. C.:  
554 Competition for water induced by transnational land acquisitions for agriculture, *Nat. Commun.*, 13(1), 505,  
555 <https://doi.org/10.1038/s41467-022-28077-2>, 2022.
- 556 Chibarabada, T., Modi, A., and Mabhaudhi, T.: Calibration and evaluation of aquacrop for groundnut (*Arachis hypogaea*) under  
557 water deficit conditions, *Agric. For. Meteorol.*, 281, 107850, <https://doi.org/10.1016/j.agrformet.2019.107850>, 2020.
- 558 CAMIYC, China Agricultural Machinery Industry Yearbook Committee: China Agricultural Machinery Industry Yearbook,  
559 China Machine Press, Beijing, 2022.
- 560 Chukalla, A. D., Krol, M. S., and Hoekstra, A. Y.: Green and blue water footprint reduction in irrigated agriculture: effect of  
561 irrigation techniques, irrigation strategies and mulching, *Hydrol. Earth Syst. Sci.*, 19, 4877-4891,  
562 <https://doi.org/10.5194/hess-19-4877-2015>, 2015.
- 563 Cui, K. and Shoemaker, S. P.: A look at food security in China, *NPJ Sci. Food.*, 2, 4, [https://doi.org/10.1038/s41538-018-0012-](https://doi.org/10.1038/s41538-018-0012-x)  
564 x, 2018.
- 565 Davis, K. F., Rulli, M. C., Seveso, A., and D'Odorico, P.: Increased food production and reduced water use through optimized  
566 crop distribution, *Nat. Geosci.*, 10(12), 919-924, <https://doi.org/10.1038/s41561-017-0004-5>, 2017.
- 567 Demay, J., Ringeval, B., Pellerin, S., and Nesme, T.: Half of global agricultural soil phosphorus fertility derived from  
568 anthropogenic sources, *Nat. Geosci.*, 16(1), 69-74, <https://doi.org/10.1038/s41561-022-01092-0>, 2023.
- 569 Dijkshoorn, K., van Engelen, V., and Huting, J.: Soil and landform properties for LADA partner countries, ISRIC report,  
570 available at: [https://data.isric.org/geonetwork/srv/eng/catalog.search#/metadata/2919b1e3-6a79-4162-9d3a-](https://data.isric.org/geonetwork/srv/eng/catalog.search#/metadata/2919b1e3-6a79-4162-9d3a-e640a1dc5aef)  
571 e640a1dc5aef. (last access: 7 March 2023), 2008.
- 572 Döll, P.: Vulnerability to the impact of climate change on renewable groundwater resources: a global-scale assessment, *Environ.*  
573 *Res. Lett.*, 4, 035006, <https://doi.org/10.1088/1748-9326/4/3/035006>, 2009.
- 574 Elliott, J., Deryng, D., Müller, C., Frieler, K., Konzmann, M., Gerten, D., Glotter, M., Flörke, M., Wada, Y., and Best, N.:  
575 Constraints and potentials of future irrigation water availability on agricultural production under climate change, *Proc.*



576 Natl. Acad. Sci. U. S. A., 111, 3239-3244, <https://doi.org/10.1073/pnas.1222474110>, 2014.

577 FAO, Food and Agriculture Organization: The State of Food and Agriculture 2020. Overcoming water challenges in agriculture.  
578 Rome. <https://doi.org/10.4060/cb1447en>, 2020.

579 FAO, Food and Agriculture Organization: FAOSTAT statistical database, available at:  
580 <https://www.fao.org/faostat/en/#data/QCL>. (last access: 7 March 2023), 2023.

581 Fader, M., Gerten, D., Thammer, M., Heinke, J., Lotze-Campen, H., Lucht, W., and Cramer, W.: Internal and external green-  
582 blue agricultural water footprints of nations, and related water and land savings through trade, *Hydrol. Earth Syst. Sci.*,  
583 15, 1641-1660, <https://doi.org/10.5194/hess-15-1641-2011>, 2011.

584 Fisher, J. B., Melton, F., Middleton, E., Hain, C., Anderson, M., Allen, R., McCabe, M. F., Hook, S., Baldocchi, D., and  
585 Townsend, P. A.: The future of evapotranspiration: Global requirements for ecosystem functioning, carbon and climate  
586 feedbacks, agricultural management, and water resources, *Water Resour. Res.*, 53, 2618-2626,  
587 <https://doi.org/10.1002/2016WR020175>, 2017.

588 Galli, A., Wiedmann, T., Ercin, E., Knoblauch, D., Ewing, B., and Giljum, S.: Integrating ecological, carbon and water footprint  
589 into a “footprint family” of indicators: definition and role in tracking human pressure on the planet, *Ecol. Indic.*, 16, 100-  
590 112, <https://doi.org/10.1016/j.ecolind.2011.06.017>, 2012.

591 Ghose, B.: Food security and food self-sufficiency in China: from past to 2050, *Food Energy Secur.*, 3, 86-95,  
592 <https://doi.org/10.1002/fes3.48>, 2014.

593 Grogan, D., Frohling, S., Wisser, D., Prusevich, A., and Glidden, S.: Global gridded crop harvested area, production, yield,  
594 and monthly physical area data circa 2015, *Sci. Data*, 9, 15, <https://doi.org/10.1038/s41597-021-01115-2>, 2022.

595 Haddeland, I., Heinke, J., Biemans, H., Eisner, S., Flörke, M., Hanasaki, N., Konzmann, M., Ludwig, F., Masaki, Y., and  
596 Schewe, J.: Global water resources affected by human interventions and climate change, *Proc. Natl. Acad. Sci. U. S. A.*,  
597 111, 3251-3256, <https://doi.org/10.1073/pnas.1222475110>, 2014.

598 Halpern, B. S., Frazier, M., Verstaen, J., Rayner, P.-E., Clawson, G., Blanchard, J. L., Cottrell, R. S., Froehlich, H. E., Gephart,  
599 J. A., Jacobsen, N. S., Kuempel, C. D., McIntyre, P. B., Metian, M., Moran, D., Nash, K. L., Többen, J., and Williams, D.  
600 R.: The environmental footprint of global food production, *Nat. Sustain.*, 5(12), 1027-1039,  
601 <https://doi.org/10.1038/s41893-022-00965-x>, 2022.

602 Harris, I., Osborn, T. J., Jones, P., and Lister, D.: Version 4 of the CRU TS monthly high-resolution gridded multivariate climate  
603 dataset, *Sci. Data*, 7, 109, <https://doi.org/10.1038/s41597-020-0453-3>, 2020.

604 He, S., Zhang, Y., Ma, N., Tian, J., Kong, D., and Liu, C.: A daily and 500 m coupled evapotranspiration and gross primary  
605 production product across China during 2000–2020, *Earth Syst. Sci. Data*, 14, 5463-5488, <https://doi.org/10.5194/essd->

14-5463-2022, 2022.

- 606
- 607 Hoekstra, A. Y.: The water footprint of modern consumer society, Routledge, London, 2013.
- 608 Hoekstra, A. Y. and Chapagain, A. K.: Water footprints of nations: water use by people as a function of their consumption  
609 pattern, *Water Resour. Manag.*, 21, 35-48, <https://doi.org/10.1007/s11269-006-9039-x>, 2006.
- 610 Hoekstra, A. Y. and Chapagain, A. K.: Globalization of water: Sharing the planet's freshwater resources, Blackwell Publishing,  
611 Oxford, 2008.
- 612 Hoekstra, A. Y. and Wiedmann, T. O.: Humanity's unsustainable environmental footprint, *Science*, 344, 1114-1117,  
613 <https://doi.org/10.1126/science.1248365>, 2014.
- 614 Hoekstra, A. Y., Chapagain, A. K., Aldaya, M. M., and Mekonnen, M. M.: The water footprint assessment manual: Setting the  
615 global standard, Routledge, London, 2011.
- 616 Hoekstra, A. Y. and Mekonnen, M. M.: The water footprint of humanity. *Proc. Natl. Acad. Sci. U. S. A.*, 109, 3232-3237,  
617 <https://doi.org/10.1073/pnas.1109936109>, 2012.
- 618 Hoogeveen, J., Faurès, J.-M., Peiser, L., Burke, J., and van de Giesen, N.: GlobWat—a global water balance model to assess  
619 water use in irrigated agriculture, *Hydrol. Earth Syst. Sci.*, 19, 3829-3844, <https://doi.org/10.5194/hess-19-3829-2015>,  
620 2015.
- 621 IFPRI, International Food Policy Research Institute: Global spatially-disaggregated crop production statistics data for 2010  
622 version 2.0, available at: <https://doi.org/10.7910/DVN/PRFF8V>. (last access: 7 March 2023), 2019.
- 623 IGSNRR, Institute of Geographic Sciences and Natural Resources Research, CAS: Resource and Environment Science and  
624 Data Center, available at: <https://www.resdc.cn/data.aspx?DATAID=274>. (last access: 7 March 2023), 2022.
- 625 Jägermeyr, J., Pastor, A., Biemans, H., and Gerten, D.: Reconciling irrigated food production with environmental flows for  
626 Sustainable Development Goals implementation, *Nat. Commun.*, 8, 15900, <https://doi.org/10.1038/ncomms15900>, 2017.
- 627 Jung, M., Reichstein, M., Ciais, P., Seneviratne, S. I., Sheffield, J., Goulden, M. L., Bonan, G., Cescatti, A., Chen, J., and De  
628 Jeu, R.: Recent decline in the global land evapotranspiration trend due to limited moisture supply, *Nature*, 467, 951-954,  
629 <https://doi.org/10.1038/nature09396>, 2010.
- 630 Leng, G., Huang, M., Tang, Q., Gao, H., and Leung, L. R.: Modeling the effects of groundwater-fed irrigation on terrestrial  
631 hydrology over the conterminous United States, *J. Hydrometeorol.*, 15, 957-972, <https://doi.org/10.1175/JHM-D-13-049.1>, 2014.
- 632
- 633 Li, Z., Feng, B., Wang, W., Yang, X., Wu, P., and Zhuo, L.: Spatial and temporal sensitivity of water footprint assessment in  
634 crop production to modelling inputs and parameters, *Agric. Water Manage.*, 271, 107805,  
635 <https://doi.org/10.1016/j.agwat.2022.107805>, 2022.

636 Lian, X., Piao, S., Huntingford, C., Li, Y., Zeng, Z., Wang, X., Ciais, P., McVicar, T. R., Peng, S., and Ottlé, C.: Partitioning  
637 global land evapotranspiration using CMIP5 models constrained by observations, *Nat. Clim. Chang.*, 8, 640-646,  
638 <https://doi.org/10.1038/s41558-018-0207-9>, 2018.

639 Liu, J., Williams, J. R., Zehnder, A. J., and Yang, H.: GEPIC—modelling wheat yield and crop water productivity with high  
640 resolution on a global scale, *Agric. Syst.*, 94, 478-493, <https://doi.org/10.1016/j.agsy.2006.11.019>, 2007.

641 Liu, X., Liu, W., Tang, Q., Liu, B., Wada, Y., and Yang, H.: Global agricultural water scarcity assessment incorporating blue  
642 and green water availability under future climate change, *Earths Future*, 10, e2021EF002567,  
643 <https://doi.org/10.1029/2021EF002567>, 2022.

644 Long, D. and Singh, V. P.: Assessing the impact of end-member selection on the accuracy of satellite-based spatial variability  
645 models for actual evapotranspiration estimation, *Water Resour. Res.*, 49, 2601-2618, <https://doi.org/10.1002/wrcr.20208>,  
646 2013.

647 Lovarelli, D., Bacenetti, J., and Fiala, M.: Water Footprint of crop productions: A review, *Sci. Total Environ.*, 548, 236-251,  
648 <https://doi.org/10.1016/j.scitotenv.2016.01.022>, 2016.

649 Lutz, A. F., Immerzeel, W. W., Siderius, C., Wijngaard, R. R., Nepal, S., Shrestha, A. B., Wester, P., and Biemans, H.: South  
650 Asian agriculture increasingly dependent on meltwater and groundwater, *Nat Clim Chang*, 12(6), 566-573,  
651 <https://doi.org/10.1038/s41558-022-01355-z>, 2022.

652 Mekonnen, M. M. and Hoekstra, A. Y.: A global and high-resolution assessment of the green, blue and grey water footprint of  
653 wheat, *Hydrol. Earth Syst. Sci.*, 14, 1259-1276, <https://doi.org/10.5194/hess-14-1259-2010>, 2010.

654 Mekonnen, M. M. and Hoekstra, A. Y.: The green, blue and grey water footprint of crops and derived crop products, *Hydrol.*  
655 *Earth Syst. Sci.*, 15, 1577-1600, <https://doi.org/10.5194/hess-15-1577-2011>, 2011.

656 Mekonnen, M. M. and Hoekstra, A. Y.: Water footprint benchmarks for crop production: A first global assessment, *Ecol. Indic.*,  
657 46, 214-223, <https://doi.org/10.1016/j.ecolind.2014.06.013>, 2014.

658 Mekonnen, M. M., and Hoekstra, A. Y.: Blue water footprint linked to national consumption and international trade is  
659 unsustainable, *Nat. Food*, 1(12), 792-800, <https://doi.org/10.1038/s43016-020-00198-1>, 2020.

660 Mialyk, O., Schyns, J. F., Booij, M. J., and Hogeboom, R. J.: Historical simulation of maize water footprints with a new global  
661 gridded crop model ACEA, *Hydrol. Earth Syst. Sci.*, 26, 923-940, <https://doi.org/10.5194/hess-26-923-2022>, 2022.

662 Middleton, N. and Thomas, D.: *World atlas of desertification: Second Edition*, Arnold, London, 1997.

663 NBSC, National Bureau of Statistics: *China Statistical Yearbook*, China Statistical Press, Beijing 2022.

664 Pastor, A., Palazzo, A., Havlik, P., Biemans, H., Wada, Y., Obersteiner, M., Kabat, P., and Ludwig, F.: The global nexus of  
665 food–trade–water sustaining environmental flows by 2050, *Nat. Sustain.*, 2, 499-507, <https://doi.org/10.1038/s41893->

666 019-0287-1, 2019.

667 Pereira, L. S., Paredes, P., Rodrigues, G. C., and Neves, M.: Modeling malt barley water use and evapotranspiration partitioning  
668 in two contrasting rainfall years. *Assessing AquaCrop and SIMDualKc models*, *Agric Water Manag*, 159, 239-254,  
669 <https://doi.org/10.1016/j.agwat.2015.06.006>, 2015.

670 Pirmoradian, N. and Davatgar, N.: Simulating the effects of climatic fluctuations on rice irrigation water requirement using  
671 AquaCrop, *Agric. Water Manage.*, 213, 97-106, <https://doi.org/10.1016/j.agwat.2018.10.003>, 2019.

672 Portmann, F. T., Siebert, S., and Döll, P.: MIRCA2000—Global monthly irrigated and rainfed crop areas around the year 2000:  
673 A new high-resolution data set for agricultural and hydrological modeling, *Glob. Biogeochem. Cycle*, 24, GB1011,  
674 <https://doi.org/10.1029/2008GB003435>, 2010.

675 Puy, A., Lo Piano, S., and Saltelli, A.: Current models underestimate future irrigated areas, *Geophys. Res. Lett.*, 47,  
676 e2020GL087360, <https://doi.org/10.1029/2020GL087360>, 2020.

677 Puy, A., Borgonovo, E., Lo Piano, S., Levin, S. A., and Saltelli, A.: Irrigated areas drive irrigation water withdrawals, *Nat.*  
678 *Commun.*, 12, 4525, <https://doi.org/10.1038/s41467-021-24508-8>, 2021.

679 Raes, D., Steduto, P., Hsiao, T., and Fereres, E.: Reference Manual, Chapter3, AquaCrop Model, Version 6.1, FAO, Rome,  
680 2018.

681 Rodell, M., Velicogna, I., and Famiglietti, J. S.: Satellite-based estimates of groundwater depletion in India, *Nature*, 460, 999-  
682 1002, <https://doi.org/10.1038/nature08238>, 2009.

683 Rosa, L., Chiarelli, D. D., Rulli, M. C., Dell'Angelo, J., and D'Odorico, P.: Global agricultural economic water scarcity, *Sci.*  
684 *Adv.*, 6, eaaz6031, <https://doi.org/10.1126/sciadv.aaz6031>, 2020.

685 Siebert, S. and Döll, P.: Quantifying blue and green virtual water contents in global crop production as well as potential  
686 production losses without irrigation, *J. Hydrol.*, 384, 198-217, <https://doi.org/10.1016/j.jhydrol.2009.07.031>, 2010.

687 SCIO, State Council Information Office: White Paper: the Grain Issue in China, available at:  
688 <http://www.scio.gov.cn/zfbps/ndhf/1996/Document/307978/307978.htm>, (last access: 7 March 2023), 1996.

689 Steffen, W., Richardson, K., Rockström, J., Cornell, S. E., Fetzer, I., Bennett, E. M., Biggs, R., Carpenter, S. R., De Vries, W.,  
690 and De Wit, C. A.: Planetary boundaries: Guiding human development on a changing planet, *Science*, 347, 1259855,  
691 <https://doi.org/10.1126/science.1259855>, 2015.

692 Tamea, S., Tuninetti, M., Soligno, I., and Laio, F.: Virtual water trade and water footprint of agricultural goods: the 1961–2016  
693 CWASI database, *Earth Syst. Sci. Data*, 13, 2025-2051, <https://doi.org/10.5194/essd-13-2025-2021>, 2021.

694 Tans, P., and Keeling, R.: Mauna Loa CO2 monthly mean data, <https://gml.noaa.gov/ccgg/trends/data.html>.

695 Tilman, D., Balzer, C., Hill, J., and Befort, B. L.: Global food demand and the sustainable intensification of agriculture, *Proc.*

- 696 Natl. Acad. Sci. U. S. A., 108, 20260-20264, <https://doi.org/10.1073/pnas.1116437108>, 2011.
- 697 Tuninetti, M., Tamea, S., Laio, F., and Ridolfi, L.: A Fast Track approach to deal with the temporal dimension of crop water  
698 footprint, *Environ. Res. Lett.*, 12, 074010, <https://doi.org/10.1088/1748-9326/aa6b09>, 2017.
- 699 Tuninetti, M., Tamea, S., D'Odorico, P., Laio, F., and Ridolfi, L.: Global sensitivity of high-resolution estimates of crop water  
700 footprint, *Water Resour. Res.*, 51, 8257-8272, <https://doi.org/10.1002/2015WR017148>, 2015.
- 701 Vanuytrecht, E., Raes, D., Steduto, P., Hsiao, T. C., Fereres, E., Heng, L. K., Vila, M. G., and Moreno, P. M.: AquaCrop: FAO's  
702 crop water productivity and yield response model, *Environ. Modell. Softw.*, 62, 351-360,  
703 <https://doi.org/10.1016/j.envsoft.2014.08.005>, 2014.
- 704 Wada, Y., Wisser, D., Eisner, S., Flörke, M., Gerten, D., Haddeland, I., Hanasaki, N., Masaki, Y., Portmann, F. T., and Stacke,  
705 T.: Multimodel projections and uncertainties of irrigation water demand under climate change, *Geophys. Res. Lett.*, 40,  
706 4626-4632, <https://doi.org/10.1002/grl.50686>, 2013.
- 707 Waha, K., Van Bussel, L., Müller, C., and Bondeau, A.: Climate-driven simulation of global crop sowing dates, *Glob. Ecol.*  
708 *Biogeogr.*, 21, 247-259, <https://doi.org/10.1111/j.1466-8238.2011.00678.x>, 2012.
- 709 Water Footprint Network.: WaterStat–water footprint statistics, available at: <https://waterfootprint.org/en/resources/waterstat/>.  
710 (last access: 7 March 2023), 2020.
- 711 Wang, W., Zhuo, L., Li, M., Liu, Y., and Wu, P.: The effect of development in water-saving irrigation techniques on spatial-  
712 temporal variations in crop water footprint and benchmarking, *J. Hydrol.*, 577, 123916,  
713 <https://doi.org/10.1016/j.jhydrol.2019.123916>, 2019.
- 714 Wang, W., Zhuo, L., Ji, X., Yue, Z., Li, Z., Li, M., Zhang, H., Gao, R., Yan, C., Zhang, P., and Wu, P.: CWFETB-China: Gridded  
715 dataset of consumptive water footprints, evaporation, transpiration, and associate benchmarks of crop production in China  
716 (2000-2018), Zenodo [data set], <https://doi.org/10.5281/zenodo.7756013>, 2023.
- 717 Wang, X., Müller, C., Elliot, J., Mueller, N. D., Ciais, P., Jägermeyr, J., Gerber, J., Dumas, P., Wang, C., and Yang, H.: Global  
718 irrigation contribution to wheat and maize yield, *Nat. Commun.*, 12, 1235, <https://doi.org/10.1038/s41467-021-21498-5>,  
719 2021.
- 720 Wu, H., Yue, Q., Guo, P., Xu, X., and Huang, X.: Improving the AquaCrop model to achieve direct simulation of  
721 evapotranspiration under nitrogen stress and joint simulation-optimization of irrigation and fertilizer schedules, *Agric.*  
722 *Water Manag.*, 266, 107599, <https://doi.org/10.1016/j.agwat.2022.107599>, 2022.
- 723 Xie, G., Han, D., Wang, X., and Lü, R.: Harvest index and residue factor of cereal crops in China, *Journal of China agricultural*  
724 *university*, 16, 1-8, 2011(in Chinese).
- 725 Yin, Y., Tang, Q., Liu, X., and Zhang, X.: Water scarcity under various socio-economic pathways and its potential effects on

726 food production in the Yellow River basin, *Hydrol. Earth Syst. Sci.*, 21, 791-804, [https://doi.org/10.5194/hess-21-791-](https://doi.org/10.5194/hess-21-791-2017)  
727 2017, 2017.

728 Yue, Z., Ji, X., Zhuo, L., Wang, W., Li, Z., and Wu, P.: Spatiotemporal responses of the crop water footprint and its associated  
729 benchmarks under different irrigation regimes to climate change scenarios in China, *Hydrol. Earth Syst. Sci.*, 26, 4637-  
730 4656, <https://doi.org/10.5194/hess-26-4637-2022>, 2022.

731 Zhang, F. and Zhu, Z.: Harvest index for various crops in China, *Scientia Agricultura Sinica*, 23, 83-87, 1990 (in Chinese).

732 Zhuo, L., Mekonnen, M. M., and Hoekstra, A. Y.: Sensitivity and uncertainty in crop water footprint accounting: a case study  
733 for the Yellow River basin, *Hydrol. Earth Syst. Sci.*, 18(6), 2219-2234, <https://doi.org/10.5194/hess-18-2219-2014>, 2014.

734 Zhuo, L., Mekonnen, M. M., and Hoekstra, A. Y.: The effect of inter-annual variability of consumption, production, trade and  
735 climate on crop-related green and blue water footprints and inter-regional virtual water trade: A study for China (1978–  
736 2008), *Water Res.*, 94, 73-85, <https://doi.org/10.1016/j.watres.2016.02.037>, 2016a.

737 Zhuo, L., Mekonnen, M. M., and Hoekstra, A. Y.: Benchmark levels for the consumptive water footprint of crop production  
738 for different environmental conditions: a case study for winter wheat in China, *Hydrol. Earth Syst. Sci.*, 20, 4547-4559,  
739 <https://doi.org/10.5194/hess-20-4547-2016>, 2016b.

740 Zhuo, L., Mekonnen, M. M., Hoekstra, A. Y., and Wada, Y.: Inter-and intra-annual variation of water footprint of crops and  
741 blue water scarcity in the Yellow River basin (1961–2009), *Adv. Water Resour.*, 87, 29-41,  
742 <https://doi.org/10.1016/j.advwatres.2015.11.002>, 2016c.